

STROJNIŠKI

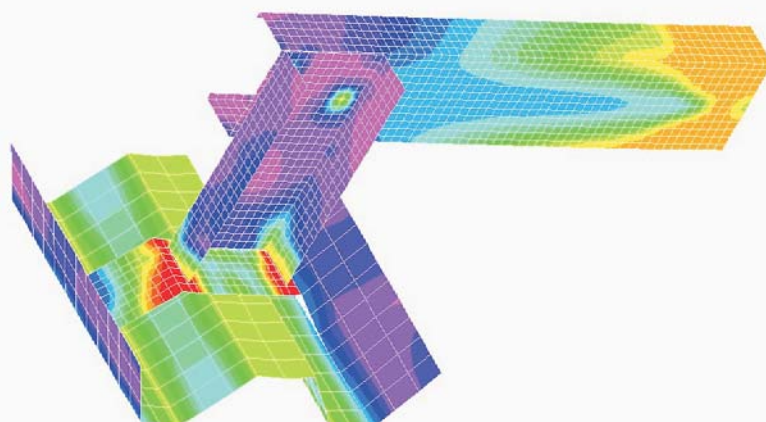
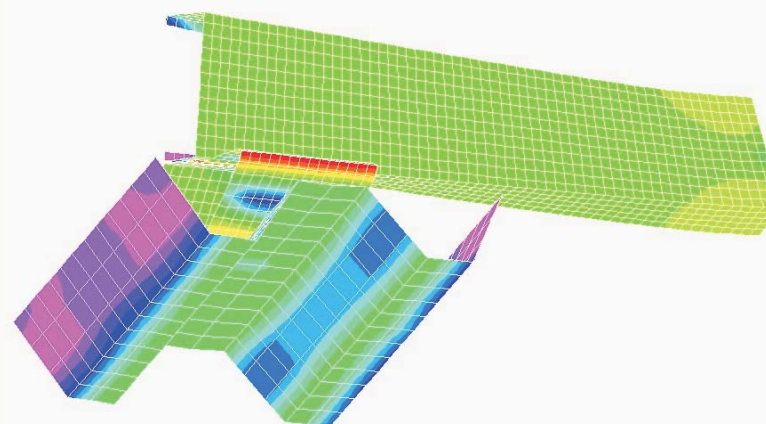
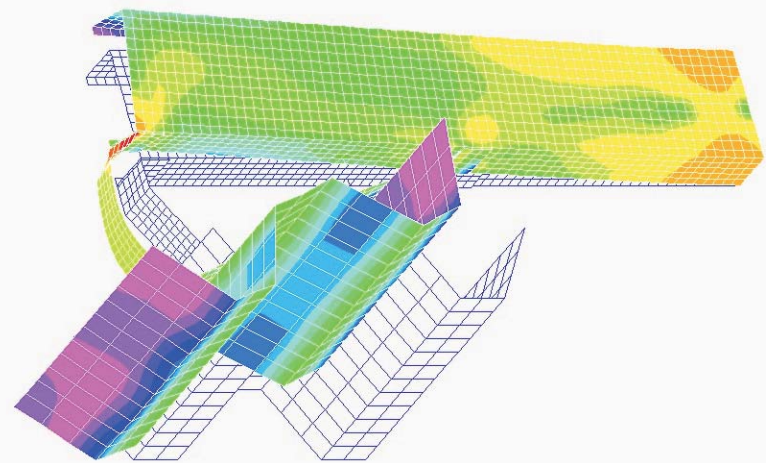
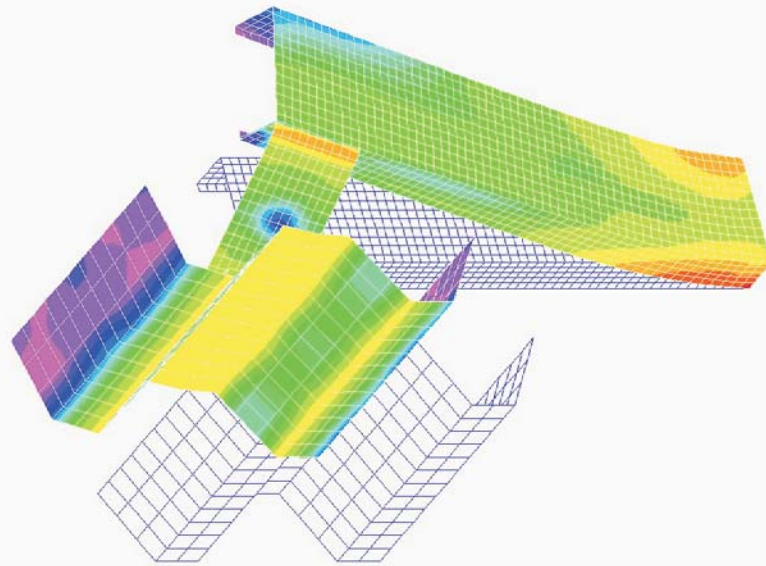
VESTNIK 10

JOURNAL OF MECHANICAL ENGINEERING

strani - pages 483 - 522

ISSN 0039-2480 . Stroj V . STJVAX

cena 800 SIT



Vsebina

Contents

Strojniški vestnik - Journal of Mechanical Engineering
letnik - volume 49, (2003), številka - number 10

Razprave

- Hočevar, M., Širok, B., Grabec, I., Rus, T.: Vpliv tlačnih utripanj v sesalni cevi na dinamiko kavitacijskega vrtinca v francisovi turbini
484
Pahole, I., Ficko, M., Drstvenšek, I., Balič, J.: Optimiranje pretoka naročil v prilagodljivih obdelovalnih sistemih z genetskimi algoritmi
499
Vesenjak, M., Ren, Z.: Računalniško podprt konstruiranje cestne varnostne ograje

Papers

- Hočevar, M., Širok, B., Grabec, I., Rus, T.: The Influence of Draft-Tube Pressure Pulsations on the Cavitation-Vortex Dynamics in a Francis Turbine
Pahole, I., Ficko, M., Drstvenšek, I., Balič, J.: Optimisation of the Flow of Orders in a Flexible Manufacturing System
Vesenjak, M., Ren, Z.: Computer-Aided Design of a Road Restraint Barrier

Osebne vesti

520 Personal Events

Navodila avtorjem

521 Instructions for Authors

Vpliv tlačnih utripanj v sesalni cevi na dinamiko kavitacijskega vrtinca v francisovi turbini

The Influence of Draft-Tube Pressure Pulsations on the Cavitation-Vortex Dynamics in a Francis Turbine

Marko Hočevar - Brane Širok - Igor Grabec - Tomaž Rus

V prispevku je predstavljen vpliv tlačnih utripanj na dinamiko kavitacijskega vrtinca v sesalni cevi francisove turbine. Pri eksperimentalnem delu na modelu francisove turbine so bila hkrati merjena utripanja tlaka na steni sesalne cevi in dinamika kavitacijskega vrtinca. Dinamika kavitacijskega vrtinca je bila merjena z metodo vizualizacije.

Predstavljena je metoda, s katero je mogoče napovedati dinamiko kavitacijskega vrtinca na podlagi izmerjenih tlačnih utripanj v eni točki na steni sesalne cevi. Uspešnost napovedi je bila v povprečju zelo dobra. Napoved dinamike kavitacijskega vrtinca je bila uspešnejša v primerih, ko je bil kavitacijski vrtinec v bližini tlačnega zaznavala.

© 2003 Strojniški vestnik. Vse pravice pridržane.

(Ključne besede: turbine francis, vrtinci kavitacijski, utripanja tlačna, vizualizacija)

The influence of pressure pulsations on the cavitation-vortex dynamics in a Francis-turbine draft tube is presented. The experiment was performed on a model Francis turbine in which pressure pulsations on the draft-tube wall and the cavitation-vortex dynamics were acquired simultaneously. The cavitation-vortex dynamics was recorded using a visualization method.

An experimental model was proposed in which the cavitation-vortex dynamics was predicted based on recorded pressure information at one point on the draft-tube wall. The performance of the model is, on average, very good. The prediction of the cavitation-vortex dynamics shows better results when the distance between the pressure sensor and the cavitation vortex is short.

© 2003 Journal of Mechanical Engineering. All rights reserved.

(Keywords: Francis turbines, vortex cavitation, pressure pulsation, visualization)

0 UVOD

Podobnost med strukturo kavitacijskega vrtinca in tlačnimi utripanji je poznana. Kljub temu je informacij o funkciji povezanosti med strukturo vrtinca in tlačnimi utripanji malo. Naš namen je napovedati povprečno svetlost in strukturo kavitacijskega vrtinca, če poznamo tlak na steni sesalne cevi francisove turbine.

Kavitacijski vrtinec v hidravličnih strojih spreminja hidrodinamiko toka, povečuje hidrodinamični upor in povzroča nihanja, še posebej pri obratovanju z delno obremenitvijo. Z vidika izdelovalcev in uporabnikov turbine je zato ugodno, če poznamo kavitacijski vrtinec v sesalni cevi turbine. V tej raziskavi želimo podati

0 INTRODUCTION

The similarity between the structure of a cavitation vortex and the pressure pulsations in a draft tube is known, but there is a lack of information about functional relations between the vortex structure and the pressure pulsations. Our goal was to predict the average image intensity and the cavitation-vortex structure, provided that the pressure in the draft-tube wall of a Francis turbine is known.

The cavitation vortex in hydraulic machines generates vibrations, increases hydrodynamic drag, changes flow hydrodynamics, especially during part-load operation. From the turbine designer's and the operator's points of view, it is therefore desirable to know whether and to what extent the cavitation vortex

mogočo rešitev tega problema. Model, ki je predstavljen v tem prispevku, omogoča napovedovanje strukture kavitacijskega vrtinca v primeru, da poznamo dinamiko spremnjanja tlaka na steni sesalne cevi. Tako oblikovan model se bo lahko uporabljal za prepoznavanje kavitacijskih režimov v sesalnih cevih vodnih turbin in njihovo prilagodljivo krmiljenje.

Napovedovanje dinamike kavitacijskega vrtinca je problem, ki ga je obravnavalo več avtorjev ([1] do [5]). Za opis pojava so bili uporabljeni numerični ([6] in [7]) ter analitični modeli ([1], [2] in [8]).

V tem prispevku smo uporabili metodo napovedi, ki je podobna razpoznavanju vzorcev razumnih bitij in temelji na statističnem modeliranju. Metoda temelji na informacijah, dobljenih s predhodnimi opazovanji istega pojava v ustreznom okolju. Informacije so predstavljene kot podatki o tlaku in strukturi kavitacijskega vrtinca. Izmerjeni in zapisani podatki so temelj za osnovne parametre statističnega modela. Tak model ima strukturo nevronske mreže (NM) [9].

Nevronska mreža deluje na dva različna načina, ki ju imenujemo učenje in napoved. Med učenjem nevronska mreža dobi eksperimentalne podatke o vhodnih in izhodnih intervalih, ki sta lahko ločena v času in prostoru. Ti skupni podatki so shranjeni v spominu nevronske mreže in tvorijo eksperimentalno osnovo modela. Med napovedjo dobi nevronska mreža samo del podatkov v vhodnem intervalu in napove podatke v izhodnem intervalu. Ker kavitacijski vrtinec v splošnem opazujemo prek meritev tlačnih utripanj na steni sesalne cevi ([1] in [2]), smo te podatke uporabili kot vhodni interval za nevronske mreže. Za krmiljenje toka nevronske mreže ponujajo možnost prilagodljivega krmiljenja, ki je preprostejši in pogojno manj občutljiv na variacije parametrov kakor običajni krmilniki [10].

V nadaljevanju prispevka bomo predstavili eksperimentalni del in metodo napovedi. Delovanje metode napovedi bomo ocenjevali s primerjavo lastnosti izmerjene in napovedane povprečne svetlosti slike kavitacijskega vrtinca in celotnih slik kavitacijskega vrtinca. Povprečne svetlosti slik uporabljamo kot merilo za delež plinske faze kavitacijskega vrtinca, celotne slike pa kot merilo za strukturo kavitacijskega vrtinca. V nadaljevanju bomo opisali povezavo med tlačnimi utripanji na steni sesalne cevi in strukturo vrtinca. Povezava bo temeljila na oblikih in utripanjih tlačnega signala. Rezultate bomo primerjali z objavljenimi rezultati parametričnega modela [11] napovedi kavitacijskega vrtinca.

is present in the draft tube of a turbine. In our investigation we wanted to provide a possible solution to this problem. The model presented here allows us to predict the cavitation vortex structure by knowing only the pressure in the draft tube. In future this could be useful in cases where the draft tube is not accessible, for example, in real power plants. A model designed in this way could be used for the detection of cavitation regimes and for adaptive control.

The prediction of cavitation-vortex dynamics is a problem that has been treated by many authors ([1] to [5]). Several numerical ([6] and [7]), or analytical ([1], [2] and [8]) models can be used to describe the phenomena and the behavior of a cavitation vortex.

We used a prediction method that is similar to the recognition of patterns by intelligent beings and based on statistical modeling. The method uses the information provided by previous observations of the same phenomenon in an equivalent environment. The information is presented as joint data about the pressure and the structure of the cavitation vortex. The recorded and stored data provide the basic parameters of the statistical model. It appears that such a model exhibits a structure of artificial neural networks (ANN) [9].

The ANN operates in two different modes: learning and prediction. During learning, the ANN obtains experimental data from the input and output intervals that can be separated in time and space. These joint data are stored in the memory of the ANN and form the experimental basis of the model. During prediction, the ANN obtains only partial data from the input interval, and predicts the data in the output interval. Since the cavitation vortex is generally observed indirectly through pressure-pulsation measurements on the draft-tube wall ([1] and [2]), we use these data as an input interval for the ANN. For flow-control applications, the ANN offers the possibility of adaptive controllers, which are simpler and potentially less sensitive to parameter variations than conventional controllers [10].

In the following sections of the paper we present the experimental arrangement and the prediction method. Then, we estimate the performance of the method by comparing the properties of the predicted and the corresponding measured average cavitation-vortex image intensities, and the entire images of the cavitation vortex. The average image intensities are used as a measure of the cavitation-vortex void fraction, while the entire images are used as a measure of the cavitation-vortex structure. The results of the prediction will be presented for several operation points. The interdependence between the pressure in the draft-tube wall and the structure of the vortex will be discussed, based on the overall structure and fluctuations of the pressure signal. The results will be compared with previously published results [11] of predicting the parametric cavitation vortex.

1 POSKUS

Poskusno delo je potekalo na modelu francisove turbine. Shema poskusa je predstavljena na sliki 1. Delovne razmere modelne turbine smo določili s spremjanjem odprtja, vrtilne frekvence in tlaka. Izbrali smo dvajset delovnih točk z različnimi pretočnimi števili, tlačnimi števili in kavitacijskimi števili.

Meritve tlačnih utripanj smo izvedli s piezoelektričnim tlačnim pretvornikom Kistler, ki je bil nameščen na steni sesalne cevi turbine in povezan z notranjostjo z izvrtino premera 4 mm. Meritve tlačnih utripanj smo posneli s 16-bitno merilno kartico National Instruments s frekvenco vzorčenja 15 kHz. Signal smo filtrirali z eliptičnim filtrom 8. reda in frekvenco 5 kHz.

Slike kavitacijskega vrtinca smo posneli s sistemom za hitro vzorčenje slik, ki je bil sestavljen iz kamere CCD DALSA CA D-1/256 in kartice za zajemanje slik IC PCI z modulom AM DIG. Ločljivost kamere je znašala 256×256 točk. Frekvenca vzorčenja je znašala 175 Hz. Skupno smo v vsaki delovni točki posneli 4400 slik. Za osvetlitev kavitacijskega vrtinca smo uporabili monokromatsko svetlobo, ki je vstopala v sesalno cev skozi okno iz poliakrilnega stekla.

Vzorčenje signala tlaka in slik smo sinhronizirali s prožilnim signalom iz merilne kartice za vzorčenje tlaka. Osi zaznavala tlaka in kamere CCD sta bili nameščeni v isti vodoravni ravnini pod kotom 90° .

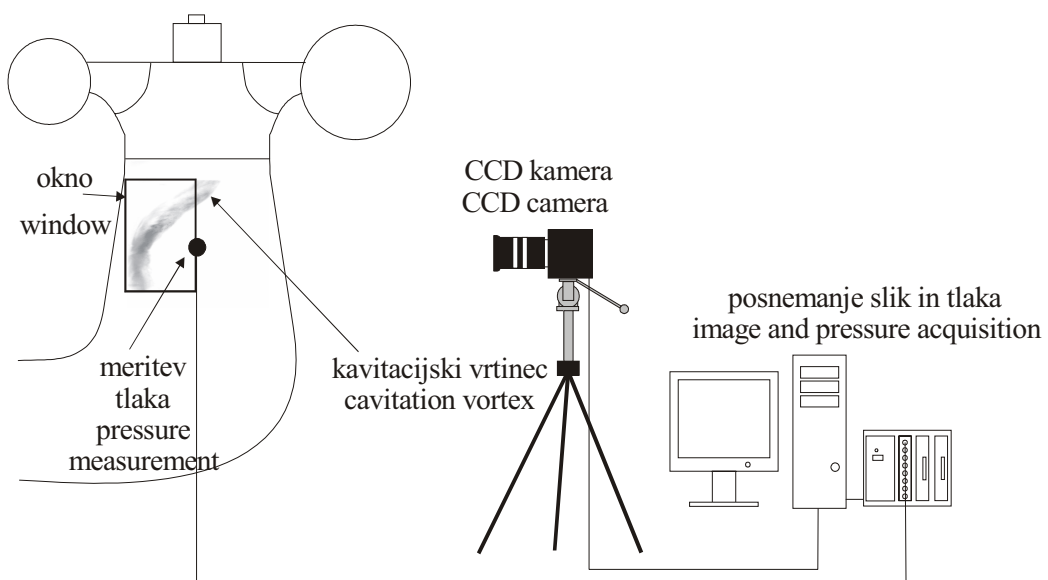
1 THE EXPERIMENT

The experimental work was performed on a model Francis-turbine test rig. The layout of the experiment is presented in Fig. 1. The operating conditions of the turbine model were set during the experiment by varying the opening, the rotation speed of the model and the pressure in the system. Twenty operation points with different flow coefficients, pressure coefficients, and cavitation numbers were selected.

The pressure was measured with a Kistler piezoelectric pressure transducer, mounted directly into the wall of the turbine draft tube and connected to the turbine flow tract through a 4-mm-diameter hole. The measured pressure signals were then transferred to a processing computer with an installed 16-bit A/D data-acquisition board from National Instruments. The bandwidth of the pressure adapter was 5 kHz, and the sampling frequency was 15 kHz (via an 8-pole elliptic filter).

Images of the cavitation vortex were acquired using a fast digital-video system composed of a CCD camera, DALSA CA D-1/256, and an IC PCI image-acquisition board with an AM DIG module. The resolution of the camera was 256×256 pixels. The frequency of the image acquisition was 175 Hz, and the camera's exposure time was 0.005 s. A total of 4400 images were recorded for each operation point. The monochrome light entering the draft tube through a Plexiglas window provided the illumination for the cavitation vortex in the draft tube.

The sampling of the pressure and video signal was synchronized with the triggering signal from the data-acquisition board used to acquire the pressure. The axes of the pressure sensor and of the CCD camera were located in the same horizontal plane at an angle of 90° .



Sl. 1. Shema poskusa
Fig. 1. The experimental set-up

1.1 Predobdelava slik

Za doseganje dobre kakovosti posnetih slik je treba zagotoviti ustrezeno namestitev kamere in sistema za osvetljevanje. To je bilo v primeru modelne francisove turbine oteženo zaradi omejenega prostora za namestitev kamere in svetilnih teles. S predhodno obdelavo slik smo zmanjšali odboje, vpliv ozadja in šuma ter izboljšali kontrast.

1.2 Povprečna svetlost slike v izbranem oknu

Povprečno svetlost slike v izbranem oknu smo izračunali iz slik po predhodni obdelavi. Izbrali smo okno velikosti 300 x 150 mm, ki je pokrivalo polovico poldnevne ravnine sesalne cevi pod rotorjem turbine, kar prikazuje slika 1. Izbrali smo okno enake velikosti kakor v [11]. Če predpostavimo, da je kinematika kavitacijskega vrtinca simetrična glede na os turbine, smo tako dosegli največji odziv optičnega signala na vrtilno gibanje kavitacijskega vrtinca v sesalni cevi. Za kvantitativno določitev obnašanja kavitacijskega vrtinca smo uvedli skalarno spremenljivko $A(t)$ [12]:

$$A(t) = \sum_{l=1}^{300} \sum_{m=1}^{150} E(l, m) \quad (1).$$

Spremenljivka $A(t)$ označuje povprečno svetlost v opazovanem oknu na sliki, posneti ob času t . E je svetlost točk s koordinato (l, m) v oknu. Ker smo uporabili 8-bitno monokromatsko kamero, so bile vrednosti spremenljivke E v območju od 0 do 255.

1.3 Stiskanje slike z diskretno valčno transformacijo (DVT)

Za nadaljnje napovedovanje celotne strukture slik kavitacijskega vrtinca z nevronskimi mrežami je bilo potrebno zaradi zmanjšanja računske obremenitve ločljivost obstoječe slike velikosti 256 x 256 točk zmanjšati. Izmed različnih možnih algoritmov smo izbrali DVT [13]. DVT ponuja prikaz slike na več nivojih ločljivosti, pri tem pa daje dobro učinkovitost stiskanja ([14] in [15]). Zaradi navedenih prednosti je stiskanje slik z DVT zelo uporabno orodje za različne znanstvene uporabe [16].

Primer uporabe algoritma DVT je prikazan na sliki 2. Ločljivost slike je bila zmanjšana iz 256 x 256 točk na 36 x 36 točk. S slike je razvidno, da se osnovne značilnosti strukture vrtinca ohranjajo, kar potrdjuje uporabnost metode.

1.1 Image pre-processing

To achieve good-quality images, proper positioning of both the camera and the illumination system is required. This is usually limited by the space around the test rig. In our case, images were pre-processed in order to eliminate reflection, background and noise, and to improve the contrast.

1.2 Average image intensity of the selected window

The average image intensity of a selected window was calculated from the filtered images. A window of 300 by 150 mm was selected, which covered half of the meridian plane of the draft tube, directly beneath the turbine rotor, as shown in Figure 1. To make possible a comparison of the results, the same size of window was used as in [11]. Assuming that the cavitation vortex kinematics was axisymmetrical, the maximum response of the optical signal on the rotational vortex movement in the draft tube was obtained. For the assessment of the quantitative behavior of the patterns within the cavitation vortex, the following integer-type scalar variable $A(t)$ was introduced [12] :

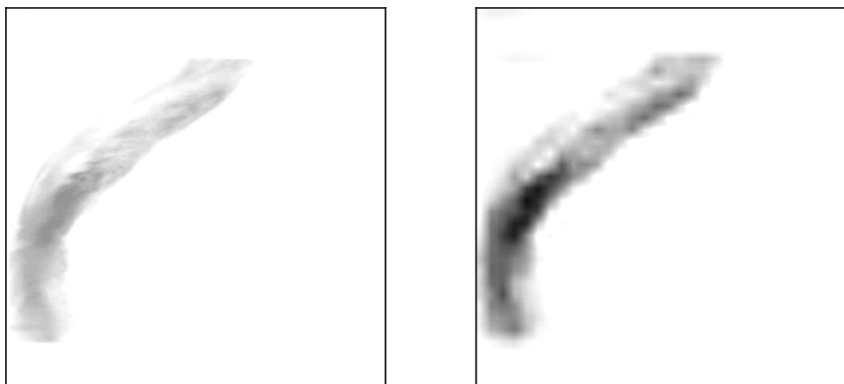
$$A(t) = \sum_{l=1}^{300} \sum_{m=1}^{150} E(l, m) \quad (1).$$

The variable $A(t)$ denotes the average intensity in the observed window in the image recorded at time t . Here, E is the intensity of pixels with spatial coordinates (l, m) inside the window. We used an 8-bit monochromatic camera, thus the values of E were in the range from 0 to 255.

1.3 Image compression using the Discrete Wavelet Transformation (DWT) algorithm

For further prediction of the entire cavitation images using neural networks, the existing image size of 256x256 pixels had to be reduced to lower the computational burden. From among various, available image-compression algorithms we chose the DWT, which has recently become popular for image-coding applications. The DWT inherently provides a multi-resolution image representation, while also improving the compression efficiency ([14] and [15]). These benefits make image compression using the DWT a very useful tool for various scientific applications [16].

A sample image showing the efficiency of the applied DWT is shown in Fig. 2. The resolution of the image was reduced from 256x256 pixels to 36x36 pixels. Figure 2 shows that the basic properties of the image are preserved, so confirming the suitability of the method.



Sl. 2. Primer slike (levo) brez stiskanja, ista slika (desno) po predobdelavi in stiskanju z DWT
Fig. 2. Sample image (left) without compression, the same image after pre-processing and DWT compression (right).

2 EKSPERIMENTALNO NAPOVEDOVANJE KAVITACIJSKEGA VRTINCA Z RADIALNIMI BAZNIMI NEVRONSKIMI MREŽAMI (RBNM)

Naravne zakone običajno opišemo kot zvezo med odvisnimi in neodvisnimi spremenljivkami $y = f(x)$. V našem primeru x pomeni neodvisni oziroma dani vektor (tlačno utripanje), medtem ko y pomeni odvisne podatke (povprečna svetlost slike oziroma slike kavitacijskega vrtinca). Osnovni problem ob tem je določiti metodo, s katero je mogoče določiti funkcijo f na podlagi danih skupnih eksperimentalnih podatkov. V ta namen smo uporabili neparametričen postopek z RBNM.

Diagram RBNM je prikazan na sliki 3. RBNM je sistem za obdelavo podatkov, sestavlja ga K spominskih celic, ki se imenujejo nevroni in imajo lokalno polje sprejemanja. To polje opisuje radialna simetrična bazna funkcija $g(x)$ vhodnega vektora x . Uporabili smo Gaussovo funkcijo $g_k(x)$ [9]:

$$g_k(x) = \exp\left(-\frac{\|x - q_k\|^2}{2\sigma_k^2}\right) \quad (2),$$

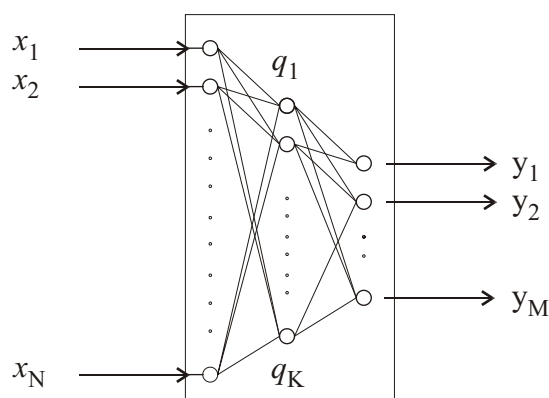
v kateri parametri q_k in σ_k označujejo središča in širino polja sprejemanja k -tega nevrona. Vsi nevroni

2 EXPERIMENTAL PREDICTION OF THE CAVITATION VORTEX USING RADIAL BASIS NEURAL NETWORKS (RBNN)

A natural law is usually described as a relationship between dependent and independent variables $y = f(x)$. In our case, x represents the independent or given data vector (pressure pulsations), while y describes the dependent data (average window intensity or cavitation-vortex images). The fundamental problem is to formulate a method by which a function f can be predicted on the basis of the joint experimental data. A non-parametric approach using RBNN was applied for this purpose.

A diagram of RBNN is shown in Fig. 3. RBNN is an information-processing system consisting of K memory cells, called neurons, with a localized receptive field. This field is described by a radially symmetrical basis function $g(x)$ of the input vector x . We employed the Gaussian function, $g_k(x)$ [9]:

in which the parameters q_k and σ_k denote the center and the width of the receptive field of the k -th



Sl. 3. Shema RBNM
Fig. 3. Diagram of the RBNN

dobijo enak vhod \mathbf{x} . Izvod $y(\mathbf{x})$ nevronske mreže je superpozicija posameznih izvodov:

$$y(\mathbf{x}) = \sum_k^K m_k g_k(\mathbf{x}) \quad (3).$$

Ta superpozicija pomeni model funkcije f , ki jo določa množica parametrov m_k , \mathbf{q}_k in σ_k . Parametre statistično ocenimo iz dane množice eksperimentalnih vzorcev (\mathbf{x}_n, y_n) , $n = 1 \dots N$, tako da je povprečno kvadratično neujemanje med izodom $y(\mathbf{x}_n)$ in eksperimentalnim podatkom y_n najmanjše:

$$E[(y(\mathbf{x}_n) - y_n)^2] \Rightarrow \min(m_k, \sigma_k, q_k) \quad (4).$$

Na voljo so številni algoritmi za zmanjšanje te kriterijske funkcije; uporabili smo algoritem, ki temelji na programskem paketu Matlab.

Pri napovedovanju smo kot vhodni vektor stanja \mathbf{x} uporabili tlak na steni sesalne cevi. Izvod y predstavlja ustrezno strukturo kavitacijskega vrtinca, ki je lahko povprečna svetlost slike ali celotna slika.

Dolžina učne množice je bila omejena na 4000 vhodno-izhodnih dvojic (\mathbf{x}, y) . Obnašanje modela smo preskusili na testni množici, ki je vsebovala 400 dvojic. Število nevronov K je bilo 2000, kar pomeni polovico števila dvojic (\mathbf{x}, y) , ki so bili uporabljeni za učenje.

Dolžino j časovno zakasnjenega vhodnega vektorja \mathbf{x} , oziroma potek tlačnih utripanj, smo uvedli v nevronske mreže z zvezko:

$$\mathbf{x} = \left(p(t), p(t - \frac{1}{f_p}), p(t - 2 \cdot \frac{1}{f_p}), \dots, p(t - j \cdot \frac{1}{f_p}) \right) \quad (5),$$

f_p je frekvenca vzorčenja tlaka p . Dolžina j časovno zakasnjenega vektorja je bila 20 vzorcev. Izbrana vrednost je omogočala najboljšo povprečno kakovost napovedi in je ustrezala približno polovici osnovne periode gibanja kavitacijskega vrtinca. Frekvenca vzorčenja tlaka f_p je bila zmanjšana na 175 Hz, kar je bilo enako frekvenci vzorčenja slik. Enake vrednosti za j in f_p smo uporabljali v vseh delovnih točkah.

3 REZULTATI IN RAZPRAVA

Vsaka delovna točka turbine vsebuje značilno dinamiko kavitacijskega vrtinca, kar vpliva na rezultate napovedovanja. Kakovost napovedovanja smo ocenjevali z regresijskimi koeficienti r_w in povprečnimi regresijskimi koeficienti \bar{r}_i . Poenostavitevne koeficiente r_w smo izračunali iz 400 zaporednih povprečnih svetlosti slik

neuron, respectivno. All neurons have the same input \mathbf{x} . The output $y(\mathbf{x})$ from the network is described by a linear superposition of the individual outputs:

This superposition represents the model of function f , which is specified by the set of parameters, m_k , \mathbf{q}_k and σ_k . These parameters are statistically estimated from a given set of experimental samples (\mathbf{x}_n, y_n) , $n = 1 \dots N$, so that the mean-square error between the network output $y(\mathbf{x}_n)$ and the experimental datum y_n is minimized:

Various algorithms for minimizing this criterion function are available; we used the algorithm based on the Matlab software package.

In our prediction, the pressure in the draft-tube wall was used as the input \mathbf{x} . The output y denotes the corresponding cavitation-vortex structure, which was either an average image intensity or an entire image.

The length of the learning set in this study was limited to 4000 (\mathbf{x}, y) input-output pairs. The behavior of the model was tested on a prediction set that included 400 sample pairs. The number of neurons, K , was set to 2000, half of the number of (\mathbf{x}, y) sample pairs used for the training.

Using length j of the time-delayed input vector \mathbf{x} , the history of pressure pulsations was introduced into the network

here f_p is the frequency of the acquired pressure, p . The length, j , of the time-delayed input vector \mathbf{x} was set to 20 samples. This value was found to provide the best average-prediction performance, and to correspond to roughly half the basic period of the cavitation-core movement. The frequency of the pressure input, f_p , was downsampled to 175 Hz, which was the same as the frequency of the image acquisition. Once the values of j and f_p were set, they were used for all operation points.

3 RESULTS AND DISCUSSION

Each operating point of the turbine possesses a characteristic dynamics of the cavitation-vortex behavior, which affects the prediction performance. The prediction performance was estimated by the regression coefficients, r_w , and the average regression coefficients, \bar{r}_i . The regression coefficients, r_w , were calculated from 400 successive, predicted average

kavitacijskega vrtinca. Poenostavitevni koeficienti r_w so primerljivi z rezultati iz [11]. Povprečni regresijski koeficienti \bar{r}_i so povprečje prek 400 zaporednih regresijskih koeficientov r_i . Poenostavitevni koeficienti r_i so dvorazsežni regresijski koeficienti med izmerjenimi in napovedanimi slikami. Poenostavitevni koeficienti r_w in \bar{r}_i so prikazani v preglednici 1.

Regresijski koeficienti r_w povprečne svetlosti slike so v območju od 0,82 do 0,99, regresijski koeficienti \bar{r}_i celotne slike pa so v območju od 0,59 do 0,88. Visoke vrednosti regresijskih koeficientov r_w in \bar{r}_i kažejo dobro napoved uporabljene metode. Iz preglednice 1 je tudi razvidno, da velja $\bar{r}_i < r_w$ za vse delovne točke. Razlog za to vidimo v visokorazsežni strukturi kavitacijskega vrtinca, ki jo napovedujemo z nižjerazsežnim signalom tlaka, merjenim zgolj v eni točki na steni sesalne cevi. Čeprav je meritev v eni točki ugodna z vidika preproste uporabe modela in morebitne uporabe v krmilne namene, lahko predpostavljamo, da je za doseganje boljših rezultatov treba zagotoviti drobnejši opis strukture kavitacijskega vrtinca. Primerjava z rezultati v [11] je prikazana na sliki 4. V obeh primerih je bila uporabljena ista modelna turbina in iste delovne točke, zato je med rezultati mogoča neposredna primerjava. Rezultati modela, predstavljenega v tem prispevku, so boljši od rezultatov, predstavljenih v [11]. S slike 4 je tudi razvidno, da imajo delovne točke z visokim regresijskim koeficientom \bar{r}_i tudi visok regresijski koeficient r_w in nasprotno. Značilna razlika med rezultati, predstavljenimi v tem prispevku, in rezultati [11] je, da so bili v delu [11] uporabljeni isti podatki za učno in testno množico, v tem prispevku pa sta bili testna in učna množica ločeni.

Poleg uspešnosti z regresijskimi koeficienti bomo ocenjevali še uspešnost napovedovanja s primerjavo časovnih vrst izmerjenih in napovedanih podatkov. To bo opisano v naslednjih dveh podpoglavljih.

Preglednica 1. Regresijski koeficienti za napovedovanje povprečne svetlosti slike (r_w) in napovedovanje celotnih slik (\bar{r}_i) kavitacijskega vrtinca

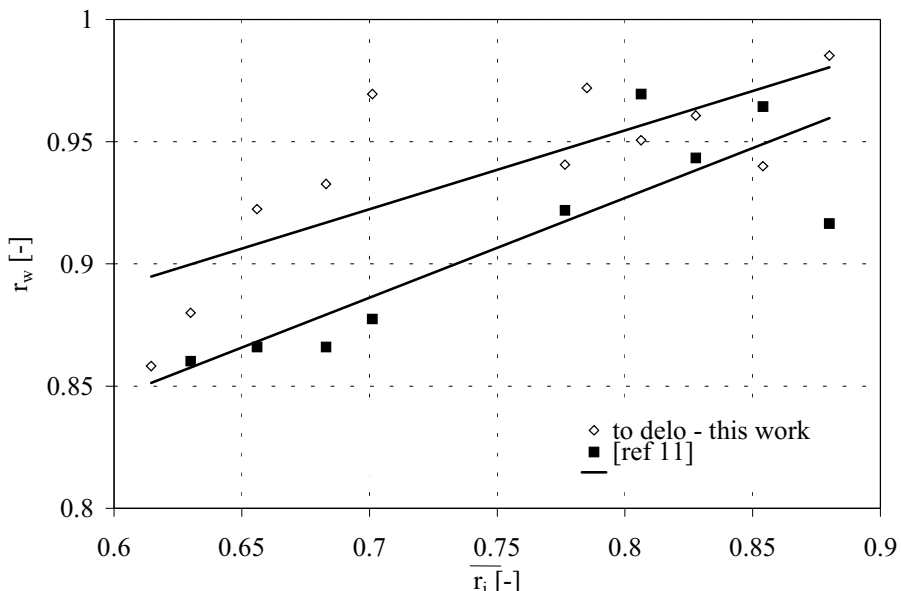
Table 1. Regression coefficients for the average image prediction (r_w) and the entire cavitation-vortex image prediction (\bar{r}_i)

delovna točka operation point	r_w	\bar{r}_i	delovna točka operation point	r_w	\bar{r}_i
1	0,90	0,76	11	0,93	0,68
2	0,91	0,75	12	0,99	0,88
3	0,97	0,70	13	0,95	0,81
4	0,95	0,79	14	0,89	0,62
5	0,97	0,79	15	0,94	0,78
6	0,88	0,62	16	0,86	0,61
7	0,92	0,66	17	0,88	0,63
8	0,82	0,61	18	0,95	0,76
9	0,96	0,85	19	0,82	0,59

intensities of the cavitation-vortex images, and are comparable with the results in [11]. The average regression coefficients, \bar{r}_i , were averaged over 400 successive regression coefficients, r_i . The regression coefficients, r_i , are two-dimensional regression coefficients between the measured and the predicted images. The regression coefficients r_w and \bar{r}_i are shown in Table 1.

The regression coefficients, r_w , of average window-intensity prediction are in the range from 0.82 to 0.99, and the regression coefficients, \bar{r}_i , of the entire image prediction are in the range from 0.59 to 0.88. The high values of the regression coefficients, r_w and \bar{r}_i , show the good prediction performance of the method. Table 1 also shows that $\bar{r}_i < r_w$ for all the operation points. The reason for this is that the high-dimensional cavitation-vortex structure is predicted by providing a lower-dimensional pressure only, and measured at only one location in the draft-tube wall. While the measurement at one point is highly desirable in terms of the model's ease of use and possible control, it can be surmised that a finer-detail description of the vortex structure would be necessary to achieve better performance. A comparison with the results in [11] is shown in Fig. 4. The same turbine and the same operation points were selected in both cases, so that a direct comparison between the two models is possible. On average, the performance of the model presented here is better than that of the model presented in [11]. Fig. 4 also shows that the operation points with high \bar{r}_i have, on average, high r_w , and vice versa. A notable difference between this work and the work performed in [11] is that in [11], the same set of data was used for the learning and the prediction, which was not the case here.

As well as using regression coefficients, we estimated the prediction performance by comparing time series of the measured and predicted data. This will be described in the next two subsections.



Sl. 4. Odvisnost regresijskih koeficientov povprečne svetlosti slike r_w od povprečnih regresijskih koeficientov napovedi celotnih slik \bar{r}_i . Eksperiment je bil izveden na isti modelni turbini in v istih delovnih točkah kakor v [11].

Fig. 4. Dependence of the regression coefficients for the average image-intensity prediction, r_w , on the regression coefficients for the entire image prediction, \bar{r}_i . The experiment in this study and in [11] were performed using the same rotor and the same operation points.

3.1 Napovedovanje povprečne svetlosti slike

V tem podpoglavlju bomo podrobnejše ocenjevali napovedovanje povprečne svetlosti slike v delovnih točkah 12, 6 in 8.

Kakovost napovedovanja za delovno točko 12 je prikazana na sliki 5 ($r_w = 0,99$). Najpomembnejša ugotovitev je dobro ujemanje med napovedanimi in izmerjenimi povprečnimi svetlostmi slike. Izmerjena in napovedana povprečna svetlost slik sta razmeroma gladki in navidezperiodični. Podobno gladko obnašanje opazimo pri tlačnih utripanjih na steni sesalne cevi, toda tlačni signali so fazno zakasnjeni v primerjavi s signalom povprečne svetlosti slike. Slika 5 kaže, da v primeru, ko je kavitacijski vrtinec blizu tlačnega zaznavala, ta zazna tlačni minimum in nasprotno. Fazni odmik med tlačnim signalom in povprečno svetlostjo slike je rezultat odmika zaradi postavitve zaznavala in izbire delovne točke [11]. Model pravilno napove fazo. Zaradi dobrega ujemanja med izmerjeno in napovedano povprečno svetlostjo slike predpostavljam, da je obnašanje kavitacijskega vrtinca v tej delovni točki navidezdeterministično.

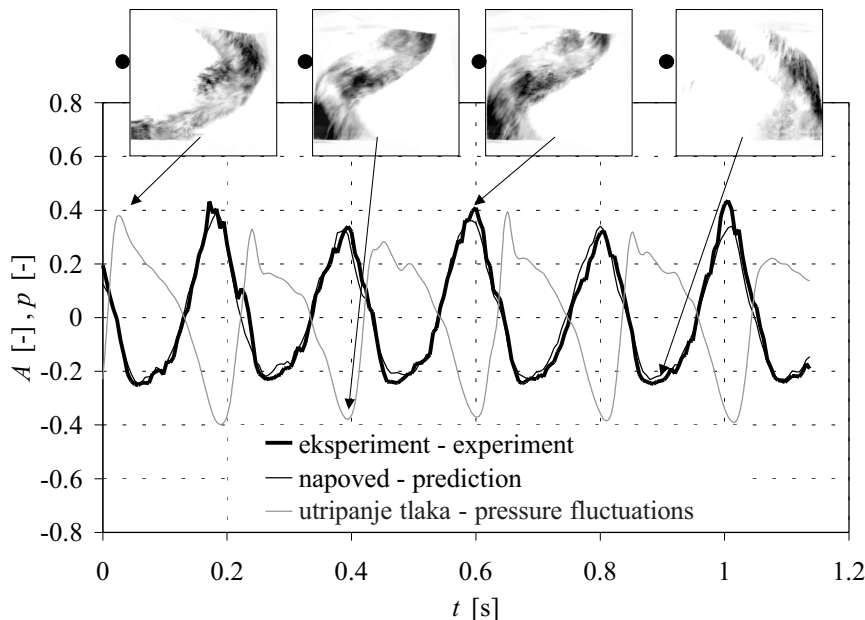
Napovedovanje v delovni točki 6 je predstavljeno na sliki 6 ($r_w = 0,88$). Ugotovili smo, da je kakovostno ujemanje med izmerjenimi in napovedanimi povprečnimi svetlostmi slik dobro celo v nekaterih visokofrekvenčnih podrobnostih. Kljub razmeroma pravilnemu gibanju

3.1 Average image-intensity prediction

In the following subsection, the performance of the average image-intensity prediction at three operation points, 12, 6 and 8, will be discussed in more detail.

The prediction performance for operation point 12 is shown in Fig. 5 ($r_w = 0.99$). The most outstanding feature here is the good agreement between the predicted average image intensities and the measured average image intensities. Both the experimental and the predicted average image intensities are relatively smooth and quasi-periodic. The same smooth behavior is observed with pressure fluctuations in the draft-tube wall, but the pressure fluctuations are phase-shifted when compared to the average image intensity. Fig. 5 shows that when the vortex is near the pressure sensor, the sensor senses a pressure minimum, and vice versa. The phase shift between the pressure signal and the average image intensity is the result of a shift due to the placement of sensors, and of the selection of the operation point [11]. The model is able to reproduce the phase correctly. From the good agreement between the experimental and predicted average image intensities we assume that the cavitation-vortex behavior at this operating point has a quasi-deterministic nature.

The prediction performance for operation point 6 is shown in Figure 6 ($r_w = 0.88$). We observed that the qualitative agreement between the measured and predicted average image intensities is good, even in some of the higher-frequency details. In spite of the relatively regular motion of the cavitation

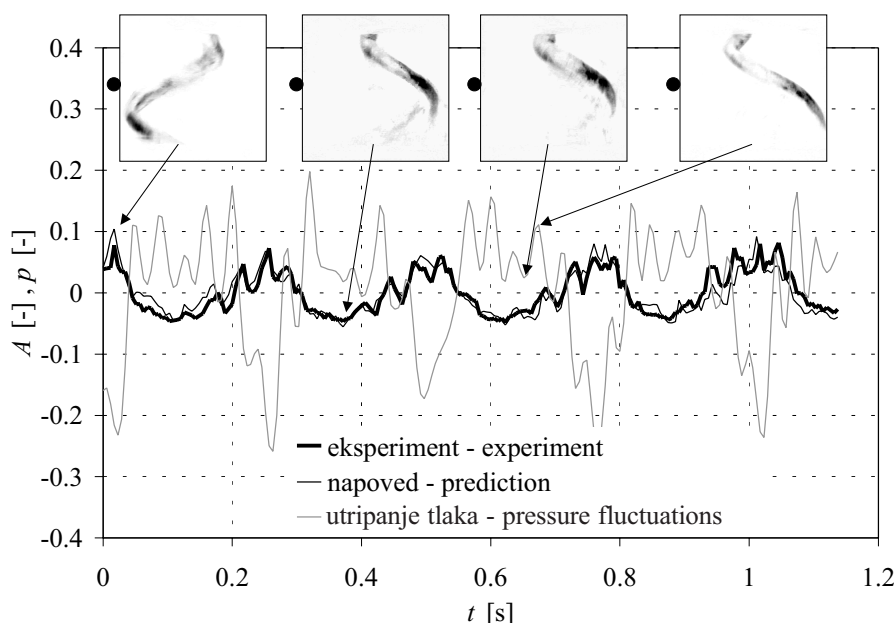


Sl. 5. Napoved povprečne svetlosti slike, delovna točka 12 ($r_w = 0,99$). Lega tlačnega zaznavala je prikazana s točko ob posamezni sliki kavitacijskega vrtinca.

Fig. 5. Prediction of the average window-intensity operation point 12 ($r_w = 0,99$). The location of the pressure sensor is shown by a dot beside each representative image.

kavitacijskega vrtinca (sl. 9, levo), lahko opazimo utriplno obnašanje povprečne svetlosti slike in tlaka na steni sesalne cevi. Močna tlačna utripanja na steni sesalne cevi kažejo na nestabilno naravo kavitacijskega vrtinca v tej delovni točki. Utriplanja so odvisna od povprečne debeline kavitacijskega vrtinca oziroma deleža plinske faze (sl. 9).

vortex (Fig. 9, left), the fluctuating behavior of the average image intensities and the pressure in the draft-tube wall can be seen. Strong pressure pulsations in the draft-tube wall indicate the unstable nature of the cavitation vortex for this operation point. These pulsations are dependent on the average vortex thickness and the cavitation-vortex void fraction (Fig. 9).



Sl. 6. Napoved povprečne svetlosti slike, delovna točka 6 ($r_w = 0,88$). Lega tlačnega zaznavala je prikazana s točko ob posamezni sliki kavitacijskega vrtinca.

Fig. 6. Prediction of the average window-intensity operation point 6 ($r_w = 0,88$). The location of the pressure sensor is shown by a dot beside each representative image.

Podobni rezultati napovedi kakor v delovni točki 6 so bili doseženi v delovni točki 8 (sl. 7, $r_w = 0,82$). V tej delovni točki kavitacijski vrtinec kaže nestabilno obnašanje (sl. 10, levo). Opazna so utripanja povprečne svetlosti slike z višjo frekvenco od osnovne, kar je povezano z utripanji tlaka. Napovedana povprečna svetlost slike se dobro ujema z izmerjeno, še posebej pri nizkih, manj pa pri visokih vrednostih povprečne svetlosti slike. Zaradi nestabilne narave tlaka v tej delovni točki tudi večja učna množica ne bi mogla izboljšati kakovosti napovedi. Velika učna množica bi prav tako zahtevala zelo dolg čas za učenje. Zaradi istega razloga nestabilne narave kavitacijskega vrtinca ni mogoče napovedati z metodami, ki temeljijo na parametričnem postopku.

Dobi rezultati, ki so prikazani na slikah 5 do 7, potrjujejo pravilno izbiro metode napovedi. Ugotovili smo, da je mogoče povprečno svetlost slike kavitacijskega vrtinca eksperimentalno napovedati, če poznamo vrednosti tlaka v izbrani točki na steni sesalne cevi. Tehnika bo lahko uporabna za ocenjevanje deleža plinske faze, če predpostavimo, da je povprečna svetlost slike sorazmerna deležu plinske faze v delu, kjer sliko povprečimo. Pri tem bo treba določiti povezavo med povprečno svetlostjo slike in deležem plinske faze.

3.2 Napoved celotnih slik

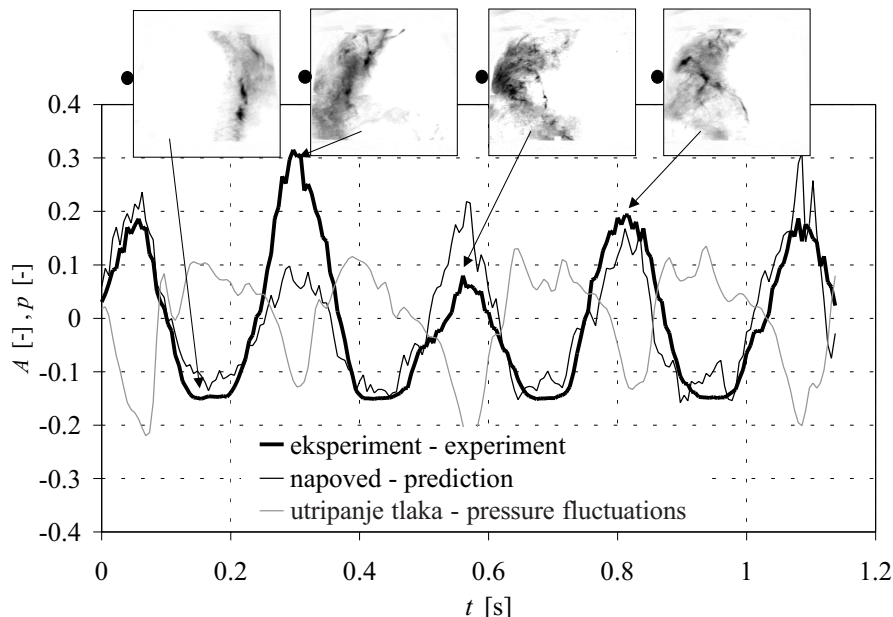
Pri napovedi celotnih slik določamo strukturo kavitacijskega vrtinca. S primerjavo izmerjenih in napovedanih slik lahko ugotovimo,

A similar prediction performance to operation point 6 was exhibited for operation point 8, shown in Fig. 7 ($r_w = 0.82$). Here, the vortex exhibits unstable behavior (Fig. 10, left). Fluctuations in the average image intensity with higher frequency than the basic frequency are present, which are related to the pressure fluctuations. The average image intensity follows the measured intensity very well, especially at low values of the average image intensity, and less at high values of the average image intensity. Because of the unstable nature of the pressure at this operation point, even a very large learning set could not improve the prediction performance. A very large learning set would also require a very long time for the learning. For the same reason, the unstable behavior of the cavitation vortex also can not be predicted using other methods, which are based on a parametric approach.

The promising results shown in Figs. 5 to 7 confirm the correct choice of prediction method. We have shown that the average image intensity of the cavitation vortex in the draft tube can be experimentally predicted using the provided pressure measurement for the selected point of the draft-tube wall. The technique could be used for an estimation of the void fraction, assuming that the average image intensity is proportional to the void-fraction volume in the region of the image where averaging is performed. However, the relation between the void fraction and the average image intensity should be established.

3.2 Entire image prediction

By predicting of entire images, the structure of the cavitation vortex is established. By comparing the measured and the predicted images one can



Sl. 7. Napoved povprečne svetlosti slike, delovna točka 8 ($r_w = 0,82$). Lega tlačnega zaznavala je prikazana s točko ob posamezni sliki kavitacijskega vrtinca.

Fig. 7. Prediction of average window-intensity operation point 8 ($r_w = 0.82$). The location of the pressure sensor is shown by a dot beside each representative image.

če časovno zakasnjeni vhodni vektor \mathbf{x} tlačnih utripanj na steni sesalne cevi vsebuje dovolj informacij za pravilno napoved celotnih slik kavitacijskega vrtinca. Model naj bi določil pravilno strukturo kavitacijskega vrtinca vključno z motnjami na lokalni skali.

Kakor v zgornjem delu bomo preučili napoved celotnih slik v delovnih točkah 12, 6 in 8. Na slikah 8, 9 in 10 so prikazane zaporedne slike kavitacijskega vrtinca, vsako zaporedje pa pomeni eno osnovno periodo gibanja. Levo zaporedje sestavlajo izmerjene slike, desno pa napovedane slike. Zaporedje teče z leve na desno in od zgoraj navzdol.

Svetlost točk na sliki je odvisna poleg strukture kavitacijskega vrtinca tudi od uporabljeni osvetlitve. Vpliv osvetlitve zaradi odbojev in senc se pojavlja periodično in je odvisen od strukture vrtinca in njegove lege v sesalni cevi, zato lahko predpostavimo, da ne poslabša kakovosti napovedi.

Rezultati napovedi v delovni točki 12 so prikazani na sliki 8 ($\bar{r}_i = 0,88$). V tej delovni točki je vrtinec razmeroma debel in stabilen. Rezultati kažejo, da je struktura kavitacijskega vrtinca napovedana pravilno, vključujuč nekatere lokalne podrobnosti.

Slika 9 prikazuje strukturo kavitacijskega vrtinca v delovni točki 6 ($\bar{r}_i = 0,62$). Kavitacijski vrtinec ima navidezperiodičen značaj. Prostornina kavitacijskega vrtinca se spreminja, to je vrtinec utripi od tanjšega k debelejšemu in nasprotno. To spremljajo utripanja tlačnega signala, prikazuje pa slika 6. Ta utripanja so glavni razlog slabše napovedi

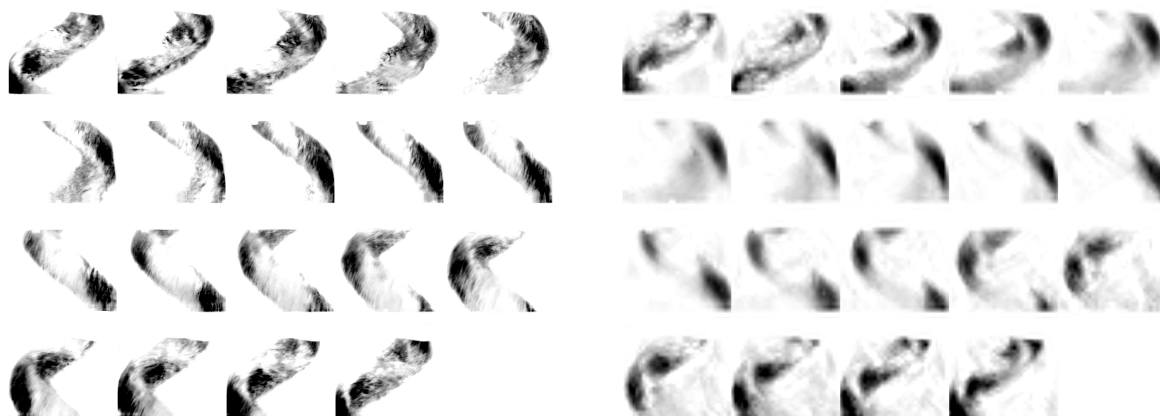
determine whether the time-delayed input vector \mathbf{x} of the pressure pulsations in the draft-tube wall contains enough information for an appropriate prediction of the entire images of the cavitation vortex. The model should determine the structure of the cavitation vortex, including perturbations on a local scale.

Again, the performance of the entire-image prediction for operation points 12, 6 and 8 will be discussed in more detail. In Figs. 8, 9 and 10, sequences of successive images of the cavitation vortex are shown, each corresponding to one period of motion. The left sections consist of the measured images, while the right sections consist of the corresponding predicted images. The sequence runs from left to right and from top to bottom.

The intensity of the image pixels of the cavitation vortex depends on its structure and on the applied illumination. Influences arising from illumination due to reflections and shadows appear regularly and depend on the vortex structure and the position in the draft tube. It is therefore our assumption that they do not deteriorate the prediction performance.

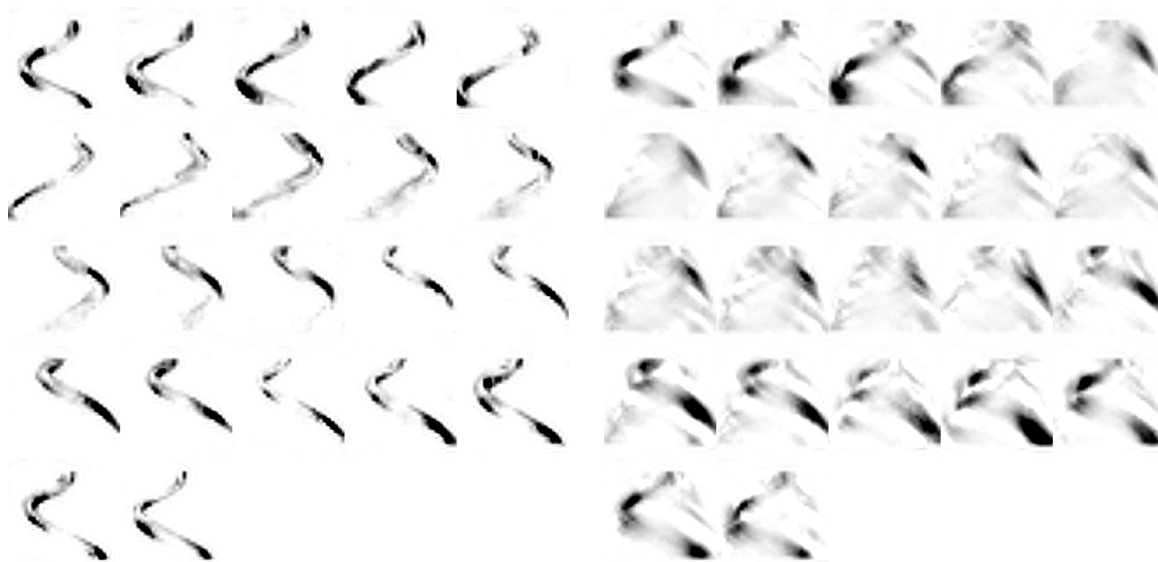
The results of the prediction of operation point 12 are shown in Fig. 8 ($\bar{r}_i = 0.88$). Here, the vortex is relatively thick and stable. The results show that the structure of the cavitation vortex is predicted fairly well, including some local details.

Fig. 9 shows the structure of the cavitation vortex for operation point 6 ($\bar{r}_i = 0.62$). The vortex has a quasi-periodic character. The volume of the cavitation vortex fluctuates, i.e. the vortex changes from thinner to thicker, and vice versa. This is accompanied by fluctuations in the pressure signal, shown in Fig. 6. These fluctuations are the main



Sl. 8. Napoved slik kavitacijskega vrtinca, delovna točka 12 ($\bar{r}_i = 0,88$). Levo : izmerjene slike, desno : napovedane slike. Časovna razlika med zaporednimi slikami je $dt = 2/175$ s. Zaporedje teče z leve na desno in od zgoraj navzdol ter pomeni eno osnovno periodo gibanja kavitacijskega vrtinca (približno 0,2 s).

Fig. 8. Prediction of the cavitation-vortex images, operation point 12 ($\bar{r}_i = 0.88$). Left: measured images, right: predicted images. The time difference between the successive images is $dt = 2/175$ s. The sequence runs from left to right and from top to bottom, and presents one period of the cavitation-vortex motion (approximately 0.2 s).



Sl. 9. Napoved slik kavitacijskega vrtinca, delovna točka 6 ($\bar{r}_i = 0,62$). Levo : izmerjene slike, desno : napovedane slike. Časovna razlika med zaporednimi slikami je $dt = 2/175$ s. Zaporedje teče z leve na desno in od zgoraj navzdol ter pomeni eno osnovno periodo gibanja kavitacijskega vrtinca (približno 0,24 s).

Fig. 9. Prediction of the cavitation-vortex images, operation point 6 ($\bar{r}_i = 0,62$). Left: measured images, right: predicted images. The time difference between the successive images is $dt = 2/175$ s. The sequence runs from left to right and from top to bottom and presents one period of the cavitation-vortex motion (approximately 0.24 s).

strukture kavitacijskega vrtinca v primerjavi z delovno točko 12 (sl. 8).

Na sliki 10 (delovna točka 8, $\bar{r}_i = 0,61$) vrtinec kaže težnjo po prehodu iz nestabilnega obnašanja turbulentnega gibanja v organiziran vzorec in nasprotno. Struktura kavitacijskega vrtinca je nestabilna, zaradi česar je kakovost napovedi značilno manjša. To je prikazano na sliki 10 v tretji vrstici.

S slik 8 do 10 lahko ugotovimo, da so bili doseženi boljši rezultati napovedi, ko je bil kavitacijski vrtinec na desni strani slike, gledano z mesta kamere. To ustrezza mestu namestitve tlačnega zaznavala, ki je bil prav tako nameščen na levi strani sesalne cevi. Boljše zaznavanje tlačnih utripanj, ki jih povzroča kavitacijski vrtinec, je bilo tako doseženo, ko je bil kavitacijski vrtinec blizu tlačnega zaznavala.

Rezultati potrjujejo, da časovno zakasnjeni vektor \mathbf{x} tlačnih utripanj vsebuje dovolj informacij za napoved celotnih slik kavitacijskega vrtinca. Metoda se je izkazala kot primerna za razumevanje in krmiljenje pojava. Kljub temu bo v prihodnosti potrebno opraviti še mnogo dela na področju osvetljevanja, predobdelave slik in parametrov nevronskeih mrež.

4 SKLEPI

V prispevku je predstavljena simultana študija kinematike kavitacijskega vrtinca in tlačnih

source of the worse prediction of the vortex structure, when compared to operation point 12 (Fig. 8).

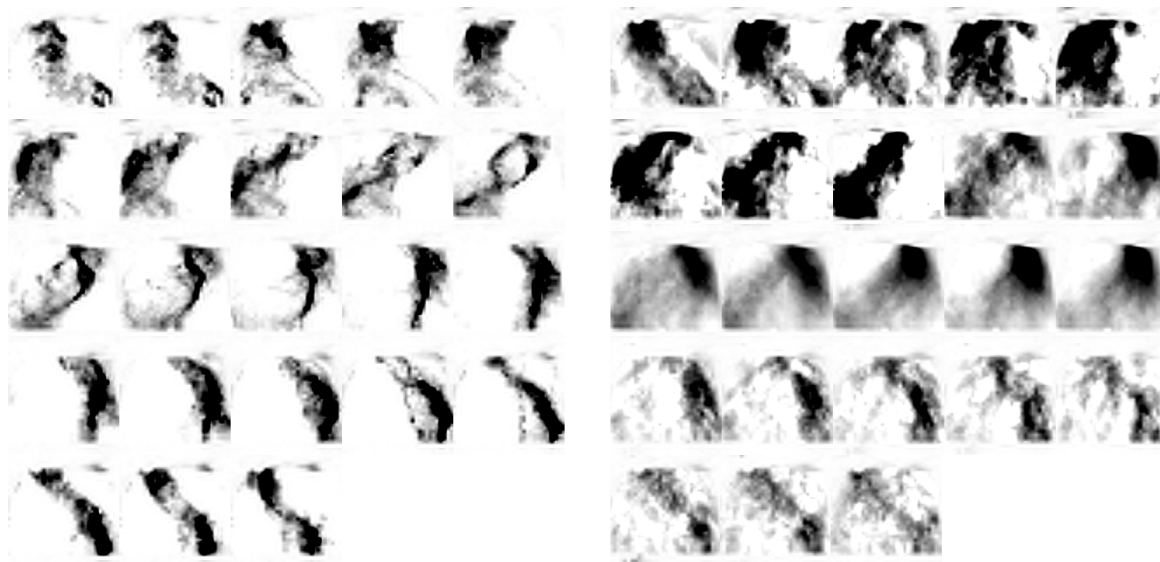
In Fig. 10 (operation point 8, $\bar{r}_i = 0,61$) the vortex shows a tendency to make a spontaneous transition from the unstable behavior of turbulent motion to an organized pattern of motion, and vice versa. The vortex structure has proven to be highly unstable and the prediction performance is significantly lower. This is shown in Fig. 10, third row.

From Figs. 8 to 10 we can see that better prediction results were achieved where the vortex was on the left-hand side of the image, as seen from the camera position. This corresponds to the mounting of the pressure sensor, which was also mounted on the left-hand side of the draft tube. Better sensing of the pressure fluctuations from the vortex was thus achieved when the vortex was close to the pressure sensor.

The presented results confirm that the time-delayed input vector \mathbf{x} of the pressure pulsations in the draft-tube wall contains enough information for a prediction of entire images of the cavitation vortex. The method has proved to be promising for understanding and controlling of the phenomenon. However, additional effort should be made in the fields of illumination, image pre-processing and prediction.

4 CONCLUSIONS

A simultaneous study of the kinematics of the cavitation-vortex core in the draft tube of a Francis turbine



Sl. 10. Napoved slik kavitacijskega vrtinca, delovna točka 6 ($\bar{r}_i = 0,61$). Levo : izmerjene slike, desno : napovedane slike. Časovna razlika med zaporednimi slikami je $dt = 2/175$ s. Zaporedje teče z leve na desno in od zgoraj navzdol ter pomeni eno osnovno periodo gibanja kavitacijskega vrtinca (približno 0,25 s).

Fig. 10. Prediction of the cavitation-vortex images, operation point 8 ($\bar{r}_i = 0,61$). Left: measured images, right: predicted images. The time difference between the successive images is $dt = 2/175$ s. The sequence runs from left to right and from top to bottom and presents one period of the cavitation-vortex motion (approximately 0.25 s).

utripanj v sesalni cevi francisove turbine. Preučili smo podobnost med izbranimi spremenljivkami in njihovo odvisnost od parametrov pojava. Rezultati potrjujejo, da časovno zakasnjeni vektor tlačnih utripanj na steni sesalne cevi vsebuje dovolj informacij za napoved povprečne svetlosti slik kavitacijskega vrtinca in strukture kavitacijskega vrtinca z uporabo radialnih baznih nevronskih mrež. Rezultati napovedi so bili v povprečju zelo dobri in se ujemajo s predhodno objavljenimi rezultati. Napoved celotnih slik kavitacijskega vrtinca je bila dobra, čeprav je bilo v točkah, v katerih je kavitacijski vrtinec nestabilen, ujemanje slabše.

V prihodnosti se kot možna uporaba kaže študija kavitacijskega vrtinca z naučeno nevronsko mrežo na podlagi umetnega vhodnega signala, kar omogoča modeliranje kinematike vrtinca v sesalni cevi in oblikovanje modelov nadzora toka v sesalnih ceveh.

Kljub dobrim rezultatom, ki so bili predstavljeni zgoraj, nekatere pomanjkljivosti tega in podobnih modelov ostajajo. Med njimi je ostalo pomanjkanje razumevanja o obnašanju kavitacijskega vrtinca v kolenu sesalne cevi. Nadaljnje delo bo potrebno za boljše razumevanje in doseganje končnega cilja, ki je krmiljenje pojava.

and the corresponding pressure pulsations was performed. The results of the study confirm the interdependence of the structural fluctuations of the vortex core and the pressure fluctuations in the draft tube. A similarity between the compared variables and their dependence on the performance parameters of the process was observed. The results of the study confirm that the time-delayed vector of pressure pulsations in the draft-tube wall carries enough information for a prediction of the average image intensity and the structure of the cavitation vortex using radial basis neural networks. The prediction performance was, on average, very good and corresponded well to the previously published results. The entire cavitation-vortex image-prediction performance was good, although in some operation points, where the vortex was unstable, the prediction performance was lower.

As a possible future study, we see the prediction of the cavitation-vortex structure using a trained network by supplying an artificial input signal for the modeling of the cavitation vortex behavior and the development of flow-control models.

In spite of the encouraging results presented above, some of the weaknesses of this and similar models remain. Among them is the lack of an interpretation of the cavitation-vortex behavior in the elbow downstream of the draft tube. Further work will thus be necessary to understand the phenomena and achieve the ultimate aim, which is to control the phenomena.

5 SIMBOLI

5 SYMBOLS

povprečna svetlost slike	A	average image intensity
svetlost točke na sliki	E	pixel intensity
funkcija	f	function
frekvenca tlaka	f_p	pressure frequency
Gaussova funkcija	g	Gaussian function
dolžina časovno zakasnjenega vhodnega vektorja	j	length of time-delayed input vector
število nevronov	K	number of neurons
koordinata točke	l	pixel coordinate
koordinata točke, uteži nevronov	m	pixel coordinate, weights of neurons
število eksperimentalnih vzorcev	N	number of experimental samples
tlačni signal	p	pressure signal
središče sprejemnega polja nevronov	\mathbf{q}	center of receptive field of neurons
regresijski koeficient povprečne svetlosti slike	r_w	average image-regression coefficient
regresijski koeficient slike	r_i	entire image-regression coefficient
povprečni regresijski koeficient slike	\bar{r}_i	average entire-image regression coefficient
čas	t	time
vhod, časovno zakasnjen tlačni vektor	\mathbf{x}	input, time-delayed pressure-pulsations vector
izhod	\mathbf{y}	output
širina sprejemnega polja nevronov	s	width of receptive field of neurons
nevronska mreža	NM/ANN	artificial neural network
osrednja procesorska enota	CPE/CPU	central processing unit
diskretna valčna transformacija	DVT/DWT	discrete wavelet transformation
radialna bazna nevronska mreža	RBNM/RBNN	radial basis neural networks

6 LITERATURA

6 REFERENCES

- [1] Fanelli, M. (1996) Some present trends in hydraulic machinery research, Proceedings of the XVIII IAHR Symposium on Hydraulic Machinery and Cavitation held in Valencia, Vol.1, *Kluwer Academic Publishers*, Dordrecht.
- [2] Fanelli, M. (1999) The cavitated »Vortex Rope« in the draft tube of Francis turbines operating at partial load: a transition from turbulent »chaos« to order?, *9th International Meeting of the IAHR Work Group on the Behaviour of Hydraulic Machinery under Steady Oscillatory Conditions*, Brno.
- [3] Brekke, H. (1999) A review on dynamic problems in Francis turbines, *9th International Meeting of the IAHR Work Group on the Behaviour of Hydraulic Machinery under Steady Oscillatory Conditions*, Brno.
- [4] Blommaert, G., J.-E. Prenat, F. Avellan, A. Boyer (1999) Active control of Francis turbine operation stability, *Proceedings of the 3rd ASME/JSME Joint Fluid Engineering Conference*, San Francisco.
- [5] Qinghua, S. (1994) Estimation of draft tube pressure pulsations for Francis turbines operating at part load conditions, *Proceedings of the XVII IAHR Symposium*, Section on Hydraulic Machinery and Cavitation, Vol.1, Beijing.
- [6] Pedrizzetti, G. (1995) A three-dimensional computational approach to the vortex rope dynamics in Francis turbine outlet, *7th International Meeting of the IAHR Work Group on the Behaviour of Hydraulic Machinery under Steady Oscillatory Conditions*, Ljubljana.
- [7] Uchiyama, T. (1998) Numerical simulation of cavitating flow using the upstream finite element method, *Applied Mathematical Modelling*, 22, 235-250.
- [8] Wang, X., M. Nishi, H. Tsukamoto (1994) A simple model for predicting the draft tube surge, *Proceedings of the XVII IAHR Symposium*, Section on Hydraulic Machinery and Cavitation, Vol.1, Beijing.
- [9] Grabec, I., W. Sachse (1997) Synergetics of measurement, prediction and control, *Springer-Verlag*, Berlin.
- [10] Gad-el-Hak, M., A. Pollard, and J.-P. Bonnet (1998) Flow control: fundamentals and practices, *Springer-Verlag*, Berlin.
- [11] Širok, B., B. Blagojević, T. Bajcar, F. Trenc, *Journal of Hydraulic Research*, in press.
- [12] Novak, M., B. Širok, M. Hočević (1999) Computer vision system as a tool for the analysis of turbulent mixing flows, *9th International Meeting of the IAHR Work Group on the Behaviour of Hydraulic*

Machinery under Steady Oscillatory Conditions, Brno.

- [13] Slavič, J., I. Simonovski, M. Boltežar (2002) Uporaba valčne transformacije pri identifikaciji dušenja nihajočih sistemov z več prostostnimi stopnjami, *Zbornik del Kuhljevi dnevi*, Ribno pri Bledu.
- [14] Rabbani, M., R. Joshi (2002) An overview of the JPEG 2000 still image compression standard, *Signal Processing: Image Communication*, 17, 3–48.
- [15] Mandala, M.K., F. Idrisa, S. Panchanathana (1999) A critical evaluation of image and video indexing techniques in the compressed domain, *Image and Vision Computing*, 17, 513–529.
- [16] Markus, H., A. Gross, L.B. Lippert, O.G. Staadt (1999) Compression methods for visualization, *Future Generation Computer Systems*, 15, 11–29.

Naslov avtorjev: mag. Marko Hočevar
doc.dr. Brane Širok
akad.prof.dr. Igor Grabec
Fakulteta za strojništvo
Univerza v Ljubljani
Aškerčeva 6
1000 Ljubljana
marko.hocevar@fs.uni-lj.si
brane.sirok@fs.uni-lj.si
igor.grabec@fs.uni-lj.si

dr. Tomaž Rus
Turboinstitut
Roušnikova 7
1210 Ljubljana - Šentvid
tomaz.rus@turboinstitut.si

Authors' Addresses: Mag. Marko Hočevar
Doc.Dr. Brane Širok
Akad.Prof.Dr. Igor Grabec
Faculty of Mechanical Eng.
University of Ljubljana
Aškerčeva 6
1000 Ljubljana, Slovenia
marko.hocevar@fs.uni-lj.si
brane.sirok@fs.uni-lj.si
igor.grabec@fs.uni-lj.si

Dr. Tomaž Rus
Turboinstitute
Roušnikova 7
1210 Ljubljana - Šentvid, Slo.
tomaz.rus@turboinstitut.si

Prejeto:
Received: 24.7.2003

Sprejeto:
Accepted: 18.12.2003

Odperto za diskusijo: 1 leto
Open for discussion: 1 year

Optimiranje pretoka naročil v prilagodljivih obdelovalnih sistemih z genetskimi algoritmi

Optimisation of the Flow of Orders in a Flexible Manufacturing System

Ivo Pahole · Mirko Ficko · Igor Drstvenšek · Jože Balic

Optimiranje pretoka naročil v prilagodljivih obdelovalnih sistemih je vedno znova zelo pereče. Poleg znanih običajnih metod optimiranja pretoka se uveljavljajo tudi nedeterministične metode. Metode optimiranja pretokov z genetskimi algoritmi spadajo med omenjene metode. V prispevku sta definirani dve prilagoditveni funkciji, ki opiseta problem optimiranja časov in stroškov izvedbe naročila. Z metodo genetskih algoritmov je nato izvedeno iskanje takšnega pretoka, da je vrednost prilagoditveni funkcij čim manjša.

© 2003 Strojniški vestnik. Vse pravice pridržane.

(Ključne besede: sistemi obdelovalni prilagodljivi, pretok naročil, optimiranje, algoritmi genetski)

In this paper we propose a method of searching for the optimum order flow through a flexible manufacturing system, with respect to transport times, preparation/completion times, manufacturing times and relevant costs. The paper defines two fitness functions describing the problem of the optimisation of times and costs of the execution of order. Then, using the genetic-algorithm method, a flow is found, such that the values of the fitness functions are as small as possible.

© 2003 Journal of Mechanical Engineering. All rights reserved.

(Keywords: flexible manufacturing systems, order flow, optimization, genetic algorithms)

0 UVOD

Pri optimiranju z znanimi običajnimi metodami je problem optimiranja pretoka naročil v prilagodljivih obdelovalnih sistemih (POS) težko obvladljiva naloga. Tako smo velikokrat prisiljeni optimirati le na eno veličino (čas izdelave, cena itn.). Poleg tega večina metod optimiranja pretoka temelji na hevrističnih metodah oblikovanja rešitve in na ekspertnem znanju izvedencev. Razlog je ta, da se pojavlja veliko različnih veličin, ki vplivajo na optimalno rešitev. Velikokrat smo prisiljeni postaviti omejitve sistema. V prispevku je opisan eden od postopkov iskanja optimalnega pretoka naročila skozi POS glede na čase prenosa, pripravno končnih časov, čase izdelave in pripadajoče stroške. Uporabljene so predpostavke, da pripravno končne čase in izdelavne čase poznamo (dobimo jih iz modulov CAPP - računalniško podprt načrtovanje postopkov). Zaradi svojih lastnosti se pri optimizacijskih problemih, kakršen je ta, izkažejo genetski algoritmi, saj lahko iščejo rešitve problemov, ki so sestavljeni iz zapletenih medsebojno odvisnih delov in bi jih bilo zelo težko modelirati [6].

0 INTRODUCTION

In addition to the well-known, conventional methods for the optimisation of order flow, also the nondeterministic methods have also become widespread. In the case of optimising with the conventional methods, the problem of optimising the orderflow in a flexible manufacturing system is a hardly controllable task. Thus, we are often restricted to optimising only one variable (the manufacturing time, the price etc). In addition, most methods for optimising the flow are based on heuristic methods of conceiving the solution and making use of the knowledge of experts. This is because there are a lot of different variables influencing the optimum solution, and we are frequently forced to set the limitations of the system. This paper describes one approach to searching for the optimum order flow through a flexible manufacturing system with respect to transport times, preparation/completion times, manufacturing times and relevant costs. The assumption is made that the preparation/completion times and the manufacturing times are known (they are obtained from CAPP - computer aided process planning, modules). Because of their properties, genetic algorithms have proved to be useful in optimisation problems like this one, since they can reach for the solutions of problems that consist of complex, mutually dependent parts, and so would be hard to model [6].

1 OPTIMIRANJE PRETOKA Z GENETSKIMI ALGORITMI

Genetske algoritme je razvil John Holland v 60. in zgodnjih 70. letih [4]. So prilagodni hevristični iskalni algoritmi, ki jih uporabljamo za reševanje zahtevnih iskalnih in optimizacijskih problemov. Ta metoda simulira razvojne postopke oziroma »preživetje najprilagojenjega« [4].

Najprej ustvarimo začetno generacijo organizmov, ki se nato z reprodukcijo, mutacijo in križanjem iz generacije v generacijo izboljšujejo. Tako dobimo postopoma vedno kakovostnejše pripadnike (organizme), ki so pravzaprav rešitve zastavljenega problema. Glavni koraki metode so:

- ustvaritev začetne generacije organizmov,
- ovrednotenje organizmov z uporabo prilagoditvene funkcije,
- izbira organizmov, ki najbolje rešijo zastavljeni problem, in
- ustvarjanje nove generacije s križanjem, reprodukcijo in mutacijo.

1.1 Prilagoditvena funkcija

Pri optimizaciji z genetskimi algoritmi moramo najprej določiti prilagoditveno funkcijo, s katero lahko ocenimo kakovost rešitev. V našem primeru je kakovostnejša tista rešitev, ki ima nižjo vrednost prilagoditvene funkcije. Uporabimo lahko tudi več prilagoditvenih funkcij naenkrat. Izbrali smo dve prilagoditveni funkciji: funkcijo spremenljivih izdelovalnih stroškov in funkcijo porabljenega časa. Glede na trenutne zahteve izbira uporabnik med temo dvema funkcijama. V proizvodnih sistemih namreč prihaja do različnih stanj. Včasih so namreč ključnega pomena stroški, včasih pa porabljen čas.

1.1.1 Iskanje najmanjših stroškov

Stroškovna funkcija je sestavljena iz treh delov. Sestavlja jo prenosni stroški naročila, pripravljalno končni stroški na posameznih strojih in čisti stroški obdelave. Tako zberemo večino spremenljivih stroškov pri izvajanju naročila:

$$\min Z = \sum_{i=1}^n \sum_{j=1}^n d_{ij} \cdot x_{ij} \cdot c_{ij} + \sum_{i=1}^n t_{pzi} \cdot y_i \cdot c_{si} + \sum_{i=1}^n \sum_{j=1}^k t_{ij} \cdot c_{si} \quad (1),$$

pri tem so:

n – število strojev v prilagodljivem obdelovalnem sistemu, d_{ij} – razdalja med strojema i in j , x_{ij} – prisotnost giba med strojema i in j pri naročilu (obstaja, ne obstaja) – vrednost je 0 ali 1, c_{ij} – stroški prenosa med strojem i in j na enoto dolžine, t_{pzi} – pripravljalno zaključni čas na stroju i , y_i – uporaba stroja i pri naročilu –

1 OPTIMISING THE FLOW BY USING GENETIC ALGORITHMS

Genetic algorithms were developed by John Holland in the 1960s and early 1970s [4]. They are adaptive, heuristic searching algorithms used for solving demanding search and optimisation problems. The genetic-algorithm method simulates evolutionary processes, or the “survival of the fittest” [4].

First, we create the initial generation of organisms, which then improve by reproduction, mutation and crossover from generation to generation. Thus, we gradually obtain members (organisms) of ever higher quality which, in fact, are the solutions to the set problem. The principal steps of the method are:

- creation of the initial generation of organisms,
- evaluation of the organisms by means of the fitness function,
- selection of the organisms that best solve the set problem,
- creation of a new generation by crossover, mutation and reproduction.

1.1 Fitness functions

In the case of optimisation by using genetic algorithms, it is necessary to first determine the fitness function, enabling the calculation of the quality of the solutions. In our case, the solution, which has a lower value of the fitness function, is of higher quality. It is also possible to use several fitness functions at one time. We selected two fitness functions: the function of the variable manufacturing costs and the function of the time spent. Taking the current requirements into account, the user selects between these two functions, because in production systems, different situations occur. Sometimes the costs are of key importance and sometimes it is the spent time.

1.1.1 Searching for the minimum costs

The cost function consists of three parts: the transport costs for the order, the preparation/completion costs on the individual machines and the net cost of the machining. In this way, the majority of the variable costs for the execution of the order are covered. The cost function is:

where:

n – number of machines in the flexible manufacturing system, d_{ij} – distance between the machine tools i and j , x_{ij} – indicates the presence of a connection between machines i and j for the order (exists, does not exist) – the value is 0 or 1, c_{ij} – transport cost between the machines i and j per unit length, t_{pzi} – preparation/completion time on machine tool i , y_i – utilization of machine tool i for the order – the value

vrednost je 0 ali 1, k – število opravil naročila, t_{ij} – tehnološki čas obdelave za stroj i in opravilo j , c_{si} – cena strojne ure za stroj i .

d_{ij} dobimo iz matrike razdalj med posameznimi stroji. Ta matrika je nespremenljiva. x_{ij} pove ali gib med strojema i in j obstaja ali ne. Dobimo ga iz genotipa organizma. c_{ij} dobimo iz matrike stroškov za povezave med strojema i in j . t_{pzi} dobimo iz CAPP modula glede na uporabljeni stroj i in naročilo. y_i dobimo iz genotipa organizma. t_{ij} dobimo iz številsko krmiljenega (ŠK - NC) programa in je odvisen od uporabljenega stroja i in operacije j .

1.1.2 Iskanje najmanjših časov

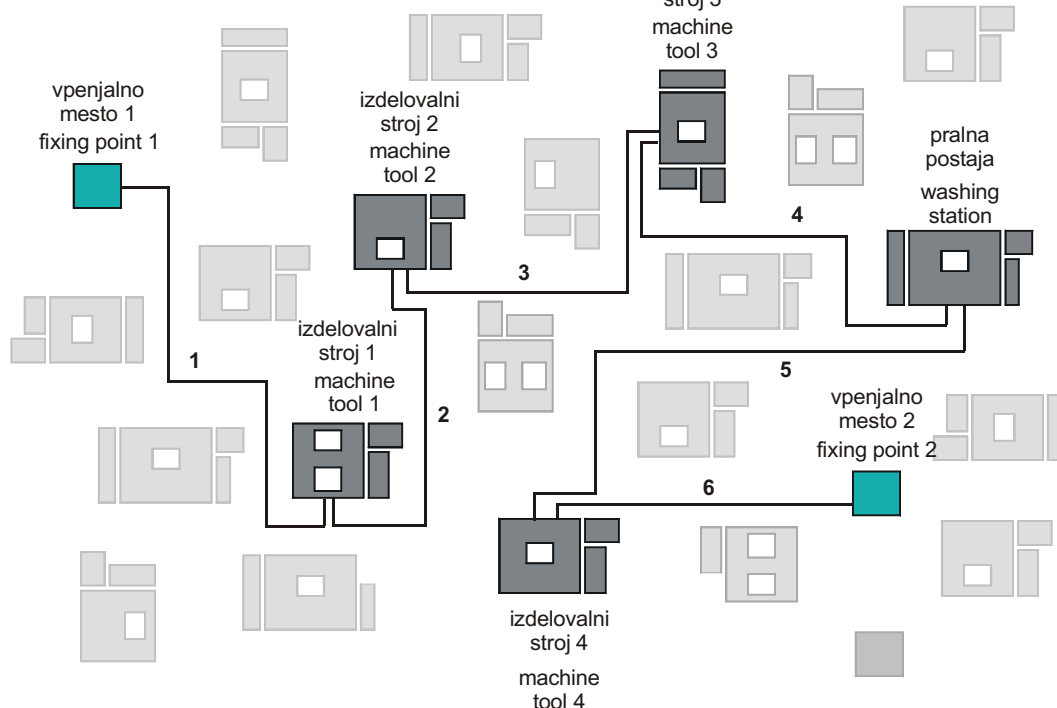
Tudi časovna funkcija je sestavljena iz treh delov in izhaja iz stroškovne funkcije.

$$\min Z = \sum_{i=1}^n \sum_{j=1}^n d_{ij} \cdot x_{ij} \cdot \frac{1}{v_{ij}} + \sum_{i=1}^n t_{pzi} \cdot y_i + \sum_{i=1}^n \sum_{j=1}^k t_{ij} \quad (2),$$

v_{ij} je hitrost prenosa med strojema i in j , v_{ij} dobimo iz matrike hitrosti posameznih prenosnih naprav.

1.2 Kodiranje

Na podlagi razčlenitve delovnega poteka na posamezna opravila in določitve strojev, na katerih se bodo posamezna opravila izvajala, določimo zaporedje pretoka (primer zaporedja pretoka prikazuje slika 1).



Sl. 1. Primer zaporedja pretoka za izpolnitev naročila
Fig. 1. Example of the sequence of flow for the execution of order

is 0 or 1, k – number of operations for the order, t_{ij} – technological time of machining for machine tool i and operation j , c_{si} – price of a machine tool hour for machine tool i .

d_{ij} is obtained from the matrix of distances between the individual machine tools. This matrix is constant. x_{ij} tells whether a connection between the machine tools i and j exists or not. It is obtained from the genotype of the organism. c_{ij} is obtained from the matrix of costs for interconnections between machine tool i and j . t_{pzi} is obtained from the CAPP module with respect to the used machine tool i and the order. y_i is obtained from the genotype of the organism. t_{ij} is obtained from the NC program and depends on the used machine tool i and the operation j .

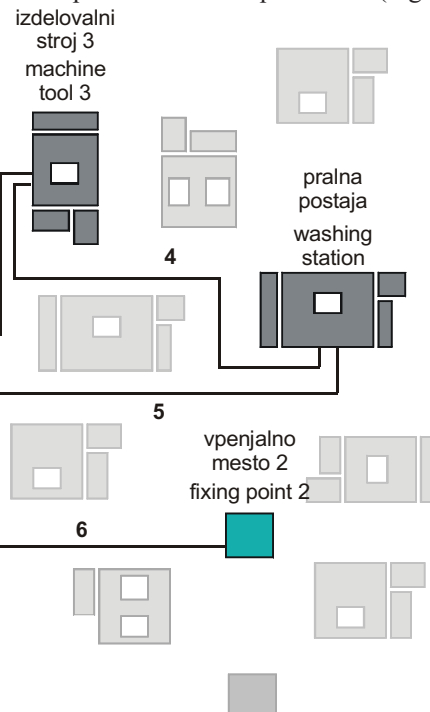
1.1.2 Searching for the minimum times

The time function also consists of three parts and is based on the cost functions.

v_{ij} is the speed of the transport between machines i and j , v_{ij} is obtained from the matrix of speeds of the individual transport devices.

1.2 Coding

The sequence of the flow is determined in accordance with the breakdown of the work progress into the individual operations and on the basis of a determination of the machine tools on which the individual operations will be performed (Fig. 1).



Organizem mora nositi informacije o tem, katera opravila se morajo izvesti, da bo naročilo izpolnjeno in na katerih strojih se morajo omenjena opravila izvesti. Organizem je tako dvorazsežna matrika, ena razsežnost matrike je enaka 2 in druga razsežnost matrike je enaka številu opravil naročila. En gen obsega eno opravilo in stroj, na katerem se opravilo izvaja. Za določanje izvedljivosti množice opravil na določenem stroju je uporabljenha metoda standardnih opravil po standardu DIN.

1.2.1 Način iskanja obdelovalnega stroja pri znanem tehnološkem postopku

Pri načrtovanju tehnologije določimo tehnološki postopek. Določimo delovna opravila, ki jih zahteva oblika in geometrijska oblika izdelka. Opravila se v glavnem opisujejo z opisnim načinom (čelno poravnati, frezati do globine itn.). Tak način opisovanja pa otežuje obdelavo s poznanimi programskimi orodji na računalnikih. V znanih standardih lahko zasledimo, da je področje opisovanja delovnih opravil zelo natančno obdelano (pregl. 1).

Takšen način označevanja delovnih opravil omogoči bistveno lažje opisovanje opravil. Tehnolog mora torej uporabiti standardni zapis. V veliko olajšanje so mu lahko grafični pripomočki na računalniku. Tako lahko kot rezultat iz modula CAPP, dobimo naslednje podatke:

- oznaka (zaporedna številka naročila) naročila za določeno obdobje načrtovanja,
- enolična oznaka naročila,
- šifra ali ime obdelovanca ali obdelovancev v naročilu,

The organisms must carry the information about which operations have to be performed for the order to be fulfilled and on which machine tools these operations must be carried out. Thus, the organism is a two-dimensional matrix: one dimension of the matrix is equal to 2 and the other dimension of the matrix is equal to the number of operations for the order. One gene comprises one operation and the machine tool on which the operation is performed. The method of standard operations according to the DIN standard is used for verifying the feasibility of the group of operations on a machine.

1.2.1 How to search for a machine tool in the case of a known technological process

During the planning of technology the technological process is determined, as are the work operations required by the shape and geometry of the product. The operations are mainly defined by a describing (to be face milled, to be milled up to a depth, etc.). Such a description, however, makes it difficult to process using known programme tools on computers. From the known standards it is possible to conclude that the area of describing the work operations has been studied very precisely (Table 1).

Designating the work operations in this way makes describing the operations considerably easier. Thus, the technologist must use the standard designations. However, graphic devices on a computer can be of great assistance to the technologist. We can obtain the following data from the CAPP module:

- designation (serial number) of the order for a certain period of planning,
- unambiguous designation of order,
- code or description of workpiece(s) in order,
- number of workpiece(s),

Preglednica 1. Primer pregleda izvedljivih delovnih opravil za obdelovalni stroj

Table 1. Example of a survey of feasible work operations for a machine tool

Pregled možnosti izvedljivih delovnih opravil za večopravilni obdelovalni stroj za vrtanje in frezanje (primer) Survey of possibilities for the execution of standard operations on a multiple-operation drilling and milling machine (example)		
Zap. št. Ser.No.	Šifra opravila po DIN 8589 Code of operation according to DIN 8589	Opis opravila za lažje razumevanje Description of operation for easier understanding
1	3.2.2.1.	skupina opravil čelnega grezenja group of operations for face sinking
2.	3.2.2.2.	skupina opravil vrtanja group of drilling operations
3.	3.2.2.3.	skupina opravil izdelave navojev v izvrtinah group of thread-cutting operations (is drilled holes)
4.
4.
7.	3.2.3.1.	plano frezanje plans milling
8.	3.2.3.2.	frezanje okroglih oblik milling of round shapes

- število obdelovancev,
- potrebni programi ŠK za določena opravila na določenih enotah,
- opis standardnih opravil po standardu DIN,
- predvideni časovni termin začetka,
- predvideni vnaprej določeni normativni čas za naročilo.

1.2.2 Določitev spektra izvedljivih opravil na obdelovalnem stroju

Za znani obdelovalni stroj lahko določimo standardna opravila, ki jih je mogoče izvesti na obdelovalnem stroju. Pod standardna opravila so mišljena opravila iz standarda DIN [3] (sl. 2). Preglednica 1 prikazuje vidno obliko datoteke za opis izvedljivih standardnih delovnih opravil na določenem obdelovalnem stroju.

V primeru, ko pa že imamo naročilo uvedeno v proizvodnjo, je velikokrat treba iskati alternativni obdelovalni stroj za določeno opravilo oziroma skupino opravil. Aktualni primeri so:

- če pride do zastoja, okvare na načrtovanem obdelovalnem stroju,
- če imamo, iz določenih drugih razlogov, proste delovne zmogljivosti na podobnih obdelovalnih strojih in želimo zmanjšati ali celo odpraviti ozko grlo;
- če se iz kakršnih koli razlogov spremeni prednost naročil (nujna naročila);
- če ni na voljo ustreznih delovnih pripomočkov ali orodij, ki so namensko vezana na določen obdelovalni stroj.

1.2.3 Izvršitev in rešitve

Želja uporabnika je gotovo avtomatizirano iskanje alternativnega obdelovalnega stroja pri izvajanju vodenja proizvodnje. Kaj hitro lahko pridemo do sklepa, popolna avtomatizacija ni

- required NC-programmes for certain operations on certain units,
- description of standard operations according to the DIN standard,
- anticipated start time,
- anticipated calculated time for order, defined in advance.

1.2.2 Determination of the spectrum of feasible operations on a machine tool

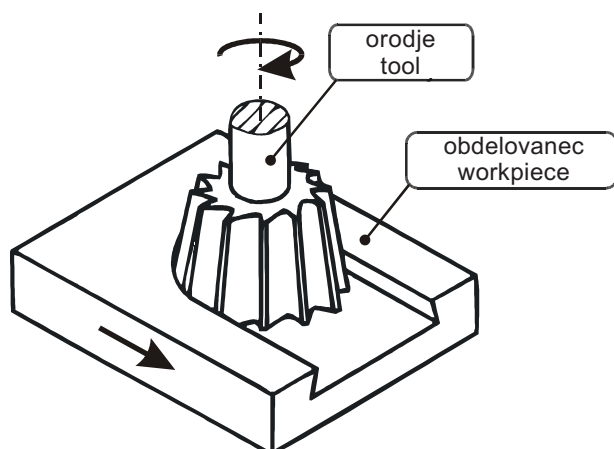
For a known machine tool it is possible to determine the standard operations that can be effected on the machine tool. The standard operations are meant to be operations defined in the DIN standard [3], (Fig. 2). Table 1 shows the visible shape of the data file for describing the feasible, standard work operations on a machine tool.

When an order has already been introduced into production, it is often necessary to search for an alternative machine tool for a certain operation or group of operations. Typical examples are:

- if stoppage, defect occurs on the planned machine tool,
- if for some other reasons there are free working capacities on similar machine tools, and a reduction or even the removal of a bottle-neck are desired,
- if for any reasons the priority of orders (urgent order) is changed,
- if proper working devices or tools, specifically connected with a certain machine tool, are not available.

1.2.3 Realisation and solutions

Automated searching for an alternative machine tool during the performance of production management is certainly the user's wish. We can come quickly to the conclusion that complete automation is



Sl. 2. Primer standardnega opravila frezanja DIN 8589, opravilo št. 3.2.3.5.1.
Fig. 2. Example of standard milling operation DIN 8589, operation No. 3.2.3.5.1.

mogoča, saj skoraj ni mogoče obdelovanca enolično opisati z ustrezno metodo ([5], [7] in [8]).

Pri iskanju rešitev prikazanega problema naletimo na več dejavnikov, od katerih je odvisna končna rešitev, če ta sploh obstaja. V sami fazi načrtovanja je mogoče izdelati več alternativnih delovnih postopkov, ki jih optimiramo glede na:

- časovno najugodnejšo ali
- ekonomsko najugodnejšo različico.

Če se poveča število teh različic delovnih postopkov postane običajno tak način načrtovanja ekonomsko vprašljiv. Lahko pa se tudi zgodi, da takega načina časovno ne zmoremo. Število mogočih različic se namreč zelo hitro povečuje [1].

Hkrati moramo pripraviti pogoje za izvajanje določenega naročila na več enotah prilagodljivega obdelovalnega sistema [8]. Še posebej velja to za tista naročila, ki imajo veliko prednost.

Za določanje oziroma izbiro alternativnega obdelovalnega stroja je lahko tehnologu operaterju velik pripomoček programska oprema »ALTER«. Izdelana programska oprema omogoča poiskati ustrezen obdelovalni stroj. Programski modul deluje tako, da primerja opravila, potrebna za izvedbo naročila, s spektrom opravil, ki jih zmorejo obdelovalni stroji. V primeru ugodne rešitve je na koncu že predviden poseg človeka, izvedenca, ki da dokončno rešitev. Slika 3 prikazuje diagram poteka programskega modula.

1.2.4 Izvedljivost naročil glede na orodja in delovne pripomočke

Izhodni podatki iz take izbire so:

- izbrano naročilo,
- obdelovalni stroj, na katerem je izbrano naročilo izvedljivo,
- delovni pripomočki, ki morajo biti na obdelovalnem stroju za izbrano naročilo,
- orodja, ki morajo biti na obdelovalnem stroju za izbrano naročilo,
- časovni čas začetka opremljanja stroja [9].

1.3 Nastanek začetne generacije

Organizem bi lahko bil sestavljen samo iz zaporedja strojev, tako da bi bil posamezni stroj zapisan tolkokrat, kolikor bi bilo na njem izvedenih opravil. Vendar pa je izvedljivost opravila neposredno vezana na stroj.

Kodiran organizem:

$$\begin{bmatrix} o_1 & o_2 & o_3 & o_4 & o_5 \\ s_1 & s_3 & s_8 & s_8 & s_2 \\ & s_4 & s_4 & s_4 & s_1 \end{bmatrix}$$

Ugotovimo, da je število pravilnih genov omejeno. Vsako opravilo lahko opravi le omejeno število strojev. To pomeni, da je število genov

not possible, since it is almost impossible to describe a workpiece by a suitable method ([5], [7] and [8]).

When searching for solutions to the problem presented across several factors by which the final solution – if it exist at all – is conditioned. During the planning stage it is possible to work out several alternative working procedures, which we optimise with regard to:

- the most favourable version with respect to time,
- the most economically favourable version.

If the number of these versions of working processes increases, such a way of planning usually becomes economically questionable. It can also happen that such a method cannot be applied because it is time-consuming [1].

In parallel, it is necessary to prepare the conditions for the execution of a certain order on several units of the flexible manufacturing system [8]. This applies particularly for orders of high priority.

The programme equipment can be of great assistance to the technologist/operator for the determination and/or selection of the alternative machine tool. The "ALTER" programme ensures that a suitable machine tool can be found. The programme module functions so that it compares the operations required for the execution of the order with the spectrum of operations that the machine tools can perform. Figure 3 shows a diagram of the flow of the programme module.

1.2.4 Feasibility of orders with respect to tools and working devices

Output data from such a selection are:

- order selected,
- machine tool on which the selected order is feasible,
- working devices that must be provided on the machine tool for the selected order,
- tools that must be available on the machine tool for the selected order,
- start time of the equipped machine [9].

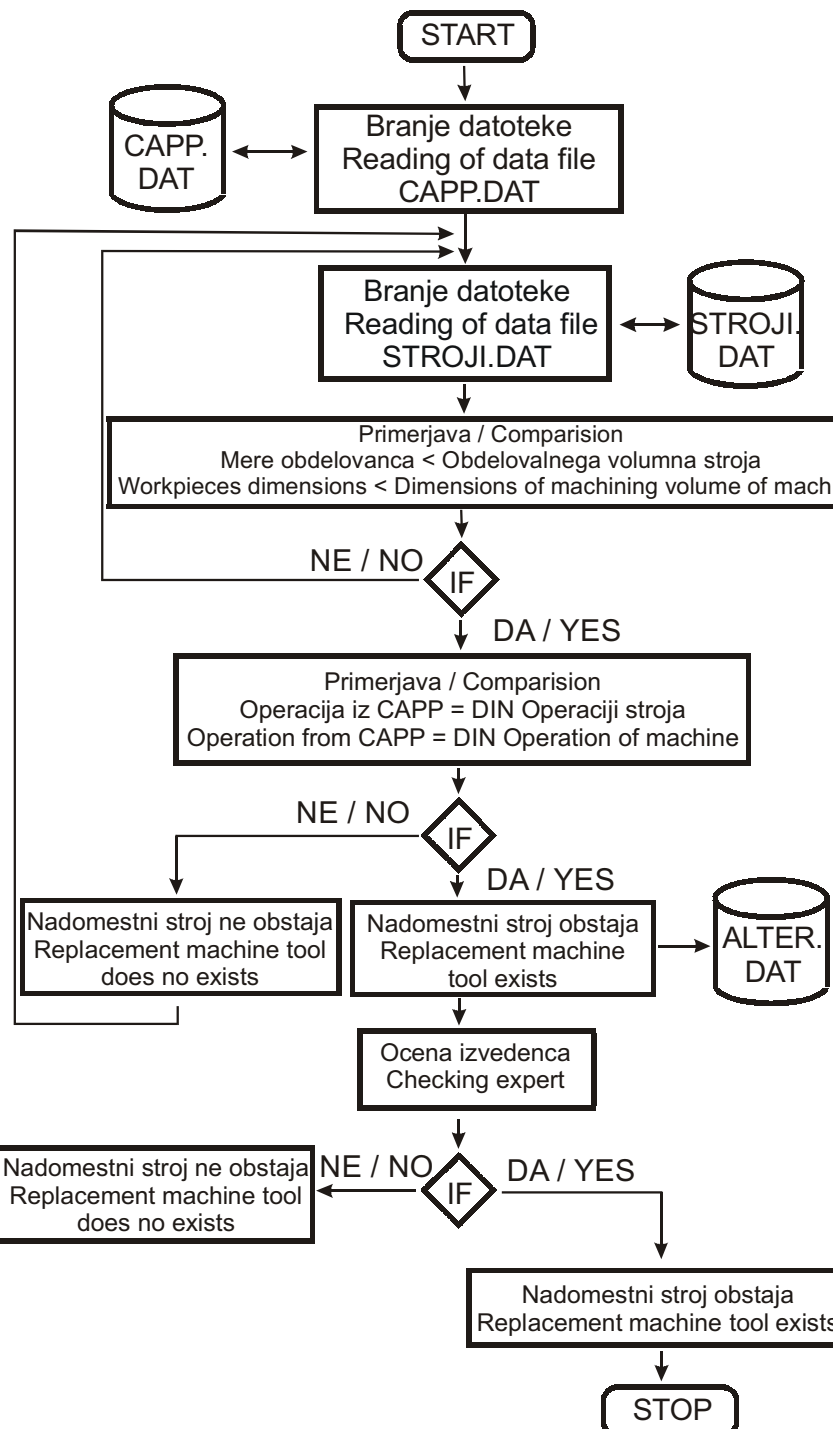
1.3 Creation of the initial generation

The organism may only consist of the sequence of machines, such that the individual machine would be mentioned so many times as the number of operations directly connected to the machine.

Coded organism:

$$\begin{bmatrix} o_6 & o_7 & o_8 & o_9 \\ s_4 & s_4 & s_4 & s_1 \end{bmatrix}$$

Each operation can be performed only by a limited number of machines, which means that the number of genes is limited. Therefore, first, all pos-



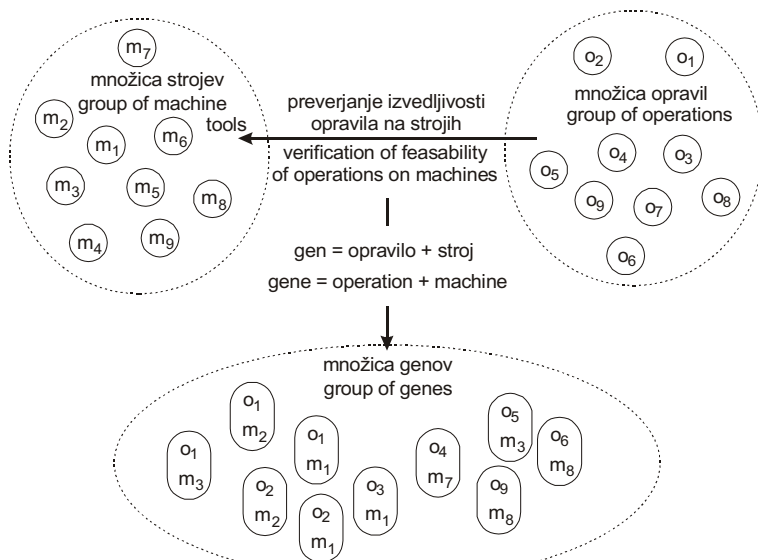
Sl. 3. Diagram poteka programskega modula »ALTER« za določanje nadomestnega obdelovalnega stroja
Fig. 3. Diagram of flow of programme module for the determination of the replacement machine tool

omejeno. Zato najprej ustvarimo vse možne gene in tako ustvarimo množico genov (sl. 4).

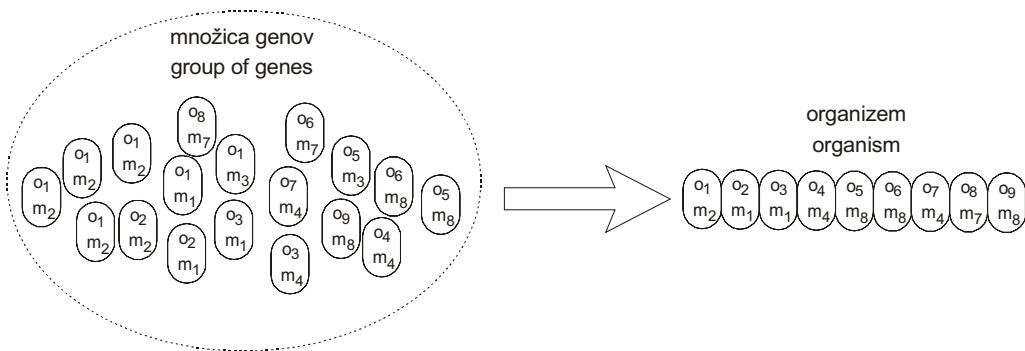
Iz te množice nato izbiramo posamezne gene in jih zlepimo skupaj v pravilne organizme (sl. 5). Pravilni organizmi so tisti, ki predstavljajo takšno zaporedje pretoka, da dobimo za rezultat izpolnjeno naročilo. Množico genov uporabimo tudi pri opravlju mutacije.

sible genes are generated and thus a group of genes is created (Fig. 4).

Out of the group, we then select the individual genes and assemble them together in correct organisms (Fig. 5). The appropriate organisms are those that represent such a sequence of the flow which results in the fulfilled order. The group of genes is also used in the operation of mutation.



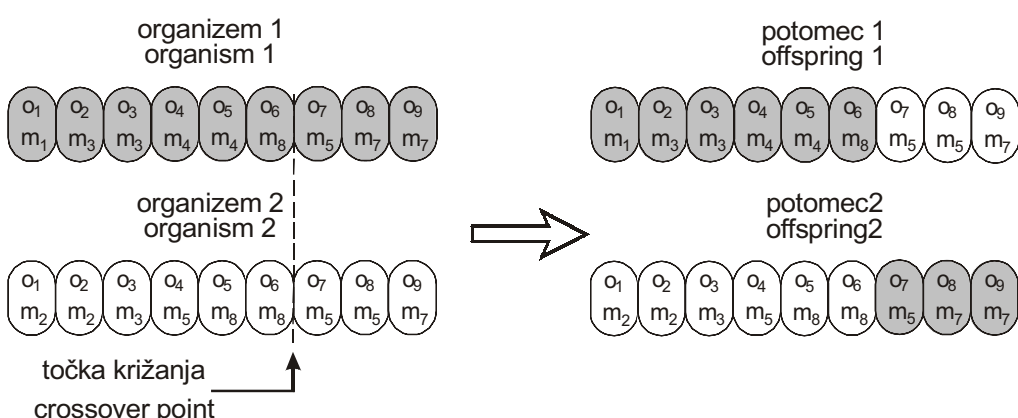
Sl. 4. Prikaz nastanka genov
Fig. 4. Representation of the coding of solutions



Sl. 5. Oblikovanje organizma iz množice genov
Fig. 5. Forming the organism from a group of genes

1.4 Razvojna in genetska opravila

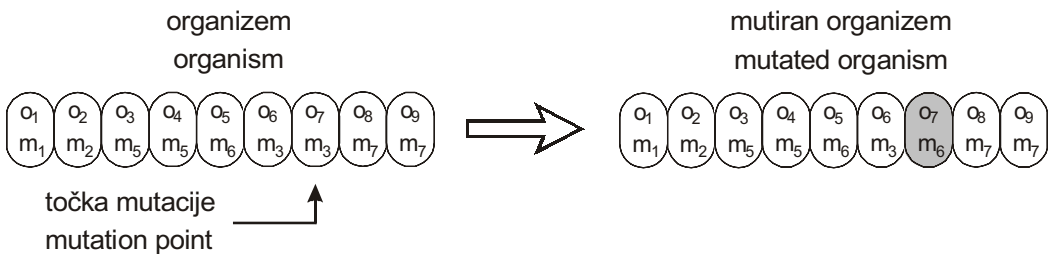
Zaradi samega načina kodiranja in ustvarjanja začetne generacije lahko uporabimo najpreprostejše enotočkovno ali večtočkovno križanje (sl. 6).



Sl. 6. Križanje organizmov
Fig. 6. Crossover of organisms

1.4 Evolutionary and genetic operations

Due to the method of coding and the generation of the initial operation, we can use the simplest single-point or multiple-point crossover (Fig. 6).



Sl. 7. Mutiranje organizmov
Fig. 7. Mutation of organisms

Prav tako kakor križanje je tudi mutacija pri tej vrsti kodiranja zelo preprosta (slika 7). Edini pogoj, ki se mora pri mutaciji upoštevati, je, da se zamenjeni geni v organizmu nadomestijo s takšnim genom, ki vsebuje enako opravilo. Nadomestni gen izberemo iz množice genov.

1.5 Ovrednotenje

Vsek organizem ovrednotimo z dvema stroškovnima funkcijama. Pri tem ima večji pomen tista stroškovna funkcija, ki je v danem trenutku za uporabnika pomembnejša. Zaporedje pretoka lahko namreč optimiramo glede na najkrajši potreben čas za izpolnitve naročila ali glede na najmanjše stroške. V primeru, da dobimo več enako dobrih rešitev glede na prvo stroškovno funkcijo, poiščemo med temi rešitvami tisto rešitev, ki najbolje reši drugo stroškovno funkcijo.

Glede na organizem se ustvarita matriki [X] in [Y], ki vsebujeta vrednosti x_{ij} in y_i in matrike tehnoloških časov $[t_p]$ in pripravljalno končnih časov $[t_{pz}]$, ki jih izdelajo moduli CAPP. Na podlagi teh matrik, ki so odvisne od samega organizma in preostalih matrik, ki so nespremenjene za postavljeno izdelavo, se izvede računanje vrednosti stroškovnih funkcij.

2 SKLEP

V nasprotju z drugimi metodami optimizacije pretoka v prilagodljivih obdelovalnih sistemih imajo genetski algoritmi nekaj neizpodbitnih prednosti. V nasprotju z večino drugih metod z genetskimi algoritmi izdelujemo rešitev po načelu naključnosti z genetskimi in evolucijskimi operacijami in ne uporabljamo nobenih pravil oblikovanja rešitve. Edina omejitev je ta, da mora biti izdelana rešitev mogoča. Kakovost izdelanih rešitev ovrednotimo s prilagoditvenima funkcijama. Pri reševanju s to metodo sicer ni nujno, da bomo dobili najboljšo rešitev, vendar bo prav gotovo med boljšimi. Prednost te metode je tudi v tem, da lahko dobimo po več zagonih genetskega algoritma več različnih rešitev, ki imajo podobno vrednost stroškovnih funkcij.

Like the crossover, the mutation is also very simple, in terms of the type of coding (Fig. 7). The sole condition to be considered in the mutation is that the genes in the organism are to be replaced by the genes containing the identical operation. The replacement gene is selected from the group of genes.

1.5 Evaluation

Each organism is evaluated by two cost functions. The cost function that is more important for the user at a given moment is of greater weight. The sequence of flow can be optimised with respect to the minimum time required for the fulfilment of the order, or with respect to the minimum cost. In the event that several solutions are equally good with respect to the first cost function obtained, from these solutions we pick the solution which best solves the other cost function.

With respect to the organism, the matrices [X] and [Y] containing the values x_{ij} and y_i are generated. The matrices of the technological times $[t_p]$ and the preparation/completion times $[t_{pz}]$, made by CAPP modules, are also generated with respect to the organism. On the basis of those matrices, depending on the organism itself and on other matrices, which are constant for the existing manufacturing, the values of the cost functions are calculated.

2 CONCLUSION

In contrast to other methods for optimising the flow in a flexible manufacturing system, genetic algorithms have a number of advantages. Unlike most other methods, with genetic algorithms we obtain solutions according to the random principle, by genetic and evolutionary operations, and we do not use any rules when conceiving the solution. The sole limitation is that the solution must be feasible. The quality of the solutions is evaluated by the two fitness functions. When solving with this method, it is not certain that the optimum solution will be obtained, but it will certainly be a better one. Another advantage of this method is that after several runs of the genetic algorithm we can obtain several different solutions with similar values for the cost functions.

3 LITERATURA
3 REFERENCES

- [1] Balič, J., Z. Živec, F. Čuš (1995) Model of a universal manufacturing interface in CIM for small-and medium sized companies. *Journal Material Processing Technology*, 52, 103-114.
- [2] Burns, R. (1997) Intelligent manufacturing. *Aircraft Engineering and Aerospace technology*, 69, 440-446.
- [3] Deutsche Normen (1981) DIN 8589 - Fertigungsverfahren Spanen, *Beuth Verlag*, Berlin.
- [4] Holland, J. (1975) Adaptation in natural and artificial systems. *University of Michigan Press*, Ann Arbor.
- [5] Katalinić, B. (1990) Industrieroboter und flexible Fertigungssysteme für Drehteile. *VDI Verlag*, Düsseldorf.
- [6] Mitchell, T. M. (1997) Machine learning. *The McGraw-Hill Companies, Inc*, New York.
- [7] Pahole, I. (1996) Using data flow matrix for small and medium-sized enterprises. *Proceedings of DAAAM - 95*, Vienna.
- [8] Pahole, I. (1997) Planiranje vodenje in optimiranje inteligentnih fleksibilnih obdelovalnih sistemov z uporabo koncepta pretočne matrike. Ph.D. thesis, *Faculty for mechanical engineering*, Maribor.
- [9] Pahole I., and J. Balič (1998) Optimization of intelligent FMS using data flow matrix method. *Proceedings of the 7th International Scientific Conference Achievements in Mechanical & Materials Engineering AMME'98*, Gliwice-Zakopane.

Naslov avtorjev: doc.dr. Ivo Pahole
mag. Mirko Ficko
dr. Igor Drstvenšek
prof.dr. Jože Balič
Univerza v Mariboru
Fakulteta za strojništvo
Smetanova 17
2000 Maribor
ivo.pahole@uni-mb.si
mirko.ficko@uni-mb.si
drsti@uni-mb.si
joze.balic@uni-mb.si

Authors' Address: Doc.Dr. Ivo Pahole
Mag. Mirko Ficko
Dr. Igor Drstvenšek
Prof.Dr. Jože Balič
University of Maribor
Faculty of Mechanical Eng.
Smetanova 17
2000 Maribor, Slovenia
ivo.pahole@uni-mb.si
mirko.ficko@uni-mb.si
drsti@uni-mb.si
joze.balic@uni-mb.si

Prejeto: 28.4.2003
Received: 28.4.2003

Sprejeto: 18.12.2003
Accepted: 18.12.2003

Odprto za diskusijo: 1 leto
Open for discussion: 1 year

Računalniško podprto konstruiranje cestne varnostne ograje

Computer-Aided Design of a Road Restraint Barrier

Matej Vesenjak - Zoran Ren

Cestne varnostne ograje na javnih cestah so namenjene za preprečitev zleta vozila s cestišča ali preboja na nasprotni vozni pas. Evropski standard SIST EN 1317 podaja merila, ki jih mora ograja izpolnjevati pod testno obremenitvijo.

Dosedanja praktična opažanja kažejo, da je sedanji distančnik cestne varnostne ograje, ki se uporablja v Republiki Sloveniji, pretog. To ima za posledico prevelike pojemetke pri naletu osebnega vozila. Zato je določitev primerne oblike distančnika izrednega pomena za povečanje varnosti udeležencev v prometu.

Namen raziskave je oblikovanje novega distančnika, ki se bo nadzorovano deformiral in bo zmožen povečati akumulacijo deformacijske energije pri naletu vozil. V ta namen so z uporabo metode končnih elementov analizirane različne oblike distančnikov. V začetni fazi razvoja je analizirana togost različnih oblik distančnikov z navidezstatično elasto-plastično analizo trirazsežnega modela odseka varnostne ograje. Ugotovljeno je, da ima sedanji distančnik zelo veliko togost in da so distančniki novih oblik zmožni večje, nadzorovane elasto-plastične deformacije pri naletu vozil.

© 2003 Strojniški vestnik. Vse pravice pridržane.

(**Ključne besede:** varnost na cestah, ograje varnostne, konstruiranje, simuliranje numerično, simuliranje nelinearno)

Road restraint barriers on public roads are used to prevent a vehicle from veering off the road or breaking through on to the opposite carriageway. The European standard SIST EN 1317 specifies the criteria that the road restraint barrier has to meet during testing.

Practical observations have shown that the distance spacer currently used in the road restraint barriers in Slovenia is too stiff. This results in too rapid decelerations during vehicle impact. Designing an improved distance spacer is therefore extremely important for increasing the safety of vehicle occupants.

The purpose of this research was to design a new distance spacer that deforms in a controllable manner and has an increased capacity for strain-energy absorption during vehicle impact. The new designs were analyzed with the finite-element method. In the initial phase of the research, the stiffness of various designs of distance spacer was analyzed using quasi-static elastic-plastic analyses of a three-dimensional road-restraint-barrier model. It was found that the currently used distance spacer is indeed much too stiff and that new distance-spacer designs are capable of larger, controllable elastic-plastic deformation during vehicle impact.

© 2003 Journal of Mechanical Engineering. All rights reserved.

(**Keywords:** roadside safety, road restraint barriers, computer aided design, numerical simulations, nonlinear simulations)

0 UVOD

Pri vedno strožjih varnostnih zahtevah in skrbi za prometno varnost so pri načrtovanju varnejših javnih cest nujno potrebne cestne varnostne ograje. Uporaba teh konstrukcij preprečuje vozilom in pešcem vstop v nevarna območja. Zaradi tega je ustrezna konstrukcija izrednega pomena.

V pripravi je slovenski pravilnik o varnostnih ograjah, ki predpisuje pogoje in načine njihove postavitve na javnih cestah. Pravilnik predpisuje,

0 INTRODUCTION

Because of increasing safety demands and concerns about road safety, road restraint barriers are of crucial importance for the planning of safer public roads. The use of these barriers prevents vehicles and pedestrians from entering into dangerous zones. Their design is therefore extremely important.

A new Slovenian technical guide for road restraint barriers is in preparation. This regulation prescribes the conditions and the methods of barrier place-

da morajo ograje ustreznati Evropskemu standardu SIST EN 1317 glede obnašanja ograje pod testno obremenitvijo [2].

Zaradi dosedanjih praktičnih ugotovitev, da ima sedanja konstrukcija cestne varnostne ograje preveliko togost, je potrebno poiskati ustrezeno rešitev, ki bo zmanjšala togost ograje in s tem pojemke pri naletu vozila ob ograjo ter tako povečala varnost potnikov v vozilu. Namen raziskave je oblikovanje novega distančnika, ki bo zmožen nadzorovane deformacije in akumulirati več deformacijske energije pri naletu vozil. Obravnavane so štiri različne oblike distančnikov.

Togost različnih oblik distančnikov je bila analizirana z navidezstatično elasto-plastično analizo trirazsežnega modela dela varnostne ograje po metodi končnih elementov.

1 OSNOVNE KONSTRUKCIJSKE ZAHTEVE VARNOSTNE OGRAJE

Namen varnostnih ograj je preprečiti zlet vozila s ceste ali preboj vozila na nasprotni vozni pas in s tem preprečiti oziroma zmanjšati poškodbe potnikov v vozilu, oseb in objektov ob vozišču, oziroma zadržati vozila, ki nenadzorovano spreminjajo smer vožnje, in jih ohraniti na ustremnem voznem pasu. Pri tem mora biti ograja zmožna akumulirati čimveč deformacijske energije, pri čemer se ne sme pretrgati.

Varnostno ograjo postavljamo na mestih, kjer je nevarnost poškodb zaradi udarca vozil v varnostno ograjo manjša od nevarnosti prehoda vozil v nevarno območje, ki je ločeno z varnostno ograjo. Na javnih cestah v Republiki Sloveniji se v skladu s spremjem evropske zakonodaje lahko postavljajo le varnostne ograje, ki so atestirane po SIST EN 1317.

Na cestah se praviloma uporablja jeklena varnostna ograja (sl. 1), v posameznih primerih pa je potrebno ali dovoljeno uporabiti tudi betonsko

ment on public roads. The regulation prescribes that the road restraint barrier's behaviour under a testing load must fulfil the European standard SIST EN 1317 [2].

Practical observations of the barriers that are currently in use indicate that the design is too stiff. Therefore, a solution has to be found that will decrease the stiffness of the road restraint barrier and thus the decelerations during vehicle impact and consequently improve the safety of vehicle occupants. The purpose of this research was to design a new distance spacer that will deform in a controlled manner and will absorb more strain energy during the vehicle impact. Four different distance-spacer designs were evaluated.

The stiffness of the various distance-spacer designs was analyzed with quasi-static elastic-plastic finite-element analyses of a three-dimensional model of a road restraint barrier.

2 BASIC DESIGN REQUIREMENTS OF THE ROAD RESTRAINT BARRIER

The purpose of a road restraint barrier is to prevent a vehicle from veering off the road or breaking through to the opposite side of the road, and so to prevent or reduce the injuries of road users and the damage caused to certain objects. The barrier also needs to be able to restrain vehicles that are changing their driving direction in an uncontrollable way and keep them on the proper side of the road. During vehicle impact the barrier has to absorb as much strain energy as possible and must not rupture.

Road restraint barriers are used in places where the danger of injuries caused by a vehicle hitting the road restraint barrier is lower than that of a vehicle veering off into a dangerous zone that is protected by a road restraint barrier. In compliance with European legalisation, only road restraint barriers that fulfil the SIST EN 1317 regulation can be used on Slovenian public roads.

The restraint barriers are usually made of steel (Fig. 1), although higher containment levels can sometimes be achieved by using concrete

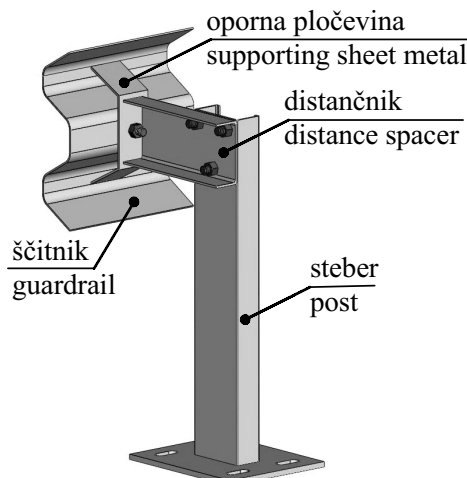


Sl. 1. Jeklena cestna varnostna ograja
Fig. 1. Steel road restraint barrier

(kadar želimo zagotoviti največjo stopnjo zadrževanja vozil) in leseno varnostno ograjo (na malo prometnih cestah iz naravovarstvenih in estetskih razlogov).

Konstrukcijski elementi jeklene cestne varnostne ograje so (sl. 2):

- ščitnik: v primeru udarca vozila s svojo deformljivo konstrukcijo zmanjša posledice udarca, pri čemer se ne sme pretrgati;
- oporna pločevina: povezuje ščitnik in distančnik, ščitniku pa daje še dodatno oporo;
- distančnik: ublaži učinek udarca vozila ob ograjo in je namenjen za povezavo med ščitnikom in stebrom ali drugo oporo;
- stebri: je nosilec distančnika in/ali ščitnika, ki zagotavlja lego ščitnika na določeni oddaljenosti od vozišča oziroma nad njim (sl. 3).



Sl. 2. Sestavni elementi cestne varnostne ograje

Fig. 2. Parts of the road restraint barrier

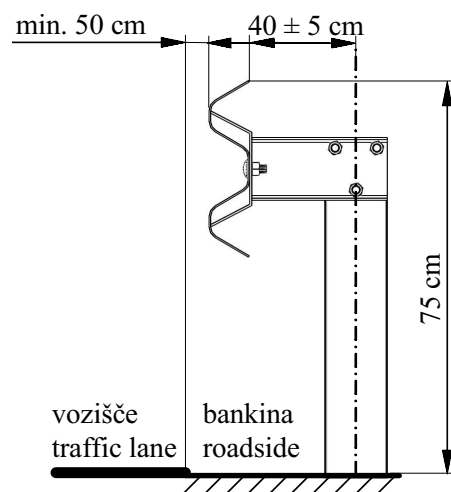
Cestne varnostne ograje so lahko eno- ali dvostranske, z distančnikom ali brez njega. Enostranska jeklena varnostna ograja je predvidena za zadrževanje vozil z ene strani (ob robovih cest), medtem ko je dvostranska ograja predvidena za zadrževanje vozil z obej strani (ločuje levi in desni pas na vozišču). Ograje z distančnikom se prvenstveno uporabljajo predvsem na avtocestah in drugih hitrih cestah, ograje brez distančnikov pa na ožjih cestah, kjer zaradi ozkih bankin ni mogoče uporabljati distančnikov.

Zgornji rob jeklene varnostne ograje mora biti postavljen 75 cm nad robom vozišča. Oddaljenost ščitnika varnostne ograje mora biti najmanj 50 cm od roba vozišča. Razdalja med ščitnikom in sredino stebra mora biti 40 ± 5 cm (sl. 3).

blocks. Wooden restraint barriers are used when a lower containment level is needed or because of nature conservation or for esthetic reasons.

Steel road restraint barriers comprise the following elements (Fig. 2):

- the guardrail: in the event of an impact the guardrail reduces the consequences with its deformable construction, although it has to be strong enough not to rupture;
- the supporting sheet metal: connects the guardrail with the distance spacer and gives the former some additional support;
- the distance spacer: decreases the severity of the impact and connects the guardrail with the post;
- the post: carries the distance spacer and/or the guardrail and ensures positioning of the guardrail at a certain distance from and above the road (Fig. 3).



Sl. 3. Mere postavitve cestne varnostne ograje

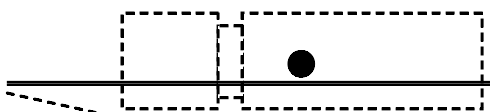
Fig. 3. Dimensions for positioning of the road restraint barrier

A road restraint barrier can be one or two-sided, with a distance spacer or without it. A one sided road restraint barrier is used to restrain a vehicle from one side (on roadsides), whereas a two-sided road restraint barrier is supposed to restrain vehicles from both sides (it separates the left-hand and the right-hand sides of the road). Distance spacers are normally used on highways and other roads with high-speed traffic, whereas guardrails without distance spacers are used in places where the space for their installation is limited.

The upper edge of the guardrail must be 75 cm above the road surface. The distance between the guardrail and the roadside must be at least 50 cm and the distance between the guardrail and the middle of the post is required to be 40 ± 5 cm (Fig. 3).

2 RAZVRSTITEV VARNOSTNIH OGRAJ PO SIST EN 1317

Naleti vozil na cestno varnostno ograjo se razlikujejo glede na maso (m), hitrost (v), kot približevanja (α), tip in obnašanje vozila ter razmere na cesti (sl. 4).



Sl. 4. Parametri teoretičnega naleta vozila
Fig. 4. Parameters of a theoretical vehicle impact

Glede na standard SIST EN 1317 so varnostne ograje razvrščene v več razredov zadrževanja vozil, pri čemer standard predpisuje kriterije, ki jih mora cestna varnostna ograja izpolniti pri določenih testnih pogojih naleta vozil.

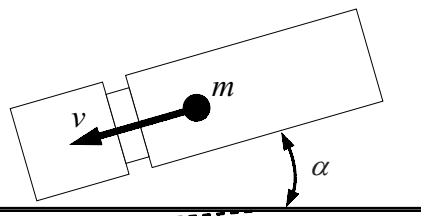
Pri tem je treba upoštevati, da mora ograja zadržati trke različnih tipov vozil, od osebnih avtomobilov do tovornjakov. Pri naletu vozil z manjšo maso (manjšo kinetično energijo), mora biti ograja nadzorovano deformabilna (mehka), da so pojemki vozila pri trku čim manjši. Pri naletu vozila z večjo maso (večjo kinetično energijo) pa mora imeti ograja dovolj veliko nosilnost, da vozilo zadrži na cestišču. Tako je pri konstruiranju cestne varnostne ograje ves čas treba iskati kompromis med togostjo (deformabilnostjo) in nosilnostjo ograje.

Cestne varnostne ograje morajo po SIST EN 1317-2 izpolnjevati naslednje kriterije:

- Stopnja zadrževanja vozil: stopnja zadrževanja različnih vrst vozil, ki je za posamezno javno cesto odvisna od njene kategorije, povprečnega letnega dnevnega prometa (PLDP), specifičnega obcestnega prostora ali nevarnega odseka ceste. Standard določa štiri stopnje zadrževanja vozil: majhno stopnjo zadrževanja (T1, T2 in T3), normalno stopnjo zadrževanja (N1 in N2), veliko stopnjo zadrževanja (H1, H2 in H3) in zelo veliko stopnjo zadrževanja (H4a in H4b). Standard predpisuje za vsako posamezno stopnjo pogoje testnega naleta vozila (masa, hitrost in kot naleta), ki jih mora cestna varnostna ograja pri trku vzdržati.
- Jakost udarca: jakost udarca vozila ob cestno varnostno ograjo v smislu ugotavljanja posledic za potnike v vozilu merimo z vrednotenjem indeksa velikosti pospeškov (IVP - ASI), z določanjem teoretične hitrosti glave pri udarcu (THGU - THIV) in z merjenjem pojemka glave

2 PERFORMANCE CLASSES OF ROAD RESTRAINT BARRIERS ACCORDING TO SISTEN 1317

Vehicle impacts on a the road restraint barrier differ in terms of the vehicle mass (m), the vehicle velocity (v), the impact angle (α), the type and behaviour of the vehicle and the road conditions (Fig. 4).



According to SIST EN 1317, road restraint barriers are divided into several performance classes of vehicle containment. The standard prescribes criteria that the road restraint barrier has to fulfil under certain test-vehicle impact conditions.

The road restraint barriers have to sustain impacts of different vehicle types (from passenger cars to trucks). In the case of a low-weight vehicle impact, the restraint barrier should deform controllably to reduce the vehicle decelerations as much as possible. However, in the case of a high-weight vehicle (higher kinetic energy) impact, the barrier must be strong enough to restrain the vehicle on the road. Thus, the design of the road restraint barrier is a compromise between its stiffness (deformability) and its strength.

Road restraint barriers have to satisfy the following criteria according to SIST EN 1317-2:

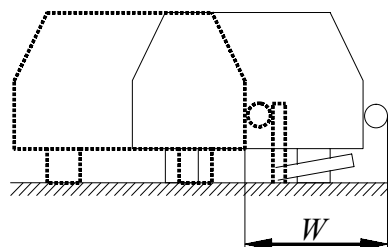
- Containment level: This represents the level of containment for different types of vehicles. The levels depend on the type of road, the average daily traffic over a year, the roadside space and dangerous road zones. The standard defines four levels of containment: the low containment level (T1, T2 and T3), the normal containment level (N1 and N2), the high containment level (H1, H2 and H3) and the very high containment level (H4a and H4b). The standard prescribes exact testing impact conditions (weight, velocity and impact angle of a vehicle) for each containment level that the road restraint barrier has to sustain in the event of an impact.
- Impact severity: The consequences of an impact for the occupants of the impacting vehicle are evaluated with the acceleration severity index (ASI), the theoretical head impact velocity (THIV) and the post-impact head deceleration (PHD). According to the standard, the limit val-

po udarcu (PGU - PHD). Glede na standard so mejne vrednosti teh parametrov naslednje: IVP $\leq 1,0$ (1,4), THGU ≤ 33 km/h in PGU ≤ 20 g.

- Deformacija cestne varnostne ograje: pomik (delovna širina) ograje (W) pomeni razdaljo med licem ščitnika varnostne ograje v prvotni legi pred naletom vozila in skrajno, od vozišča odmaknjeno točko na ograji po naletu vozila na ograjo (sl. 5). Standard navaja 8 deformacijskih razredov varnostne ograje (W1 do W8).

ues of these parameters are: ASI ≤ 1.0 (1,4), THIV ≤ 33 km/h and PHD ≤ 20 g.

- Deformation of the restraint barrier: The working width of the restraint barrier (W) is the distance between the road-face of the W-beam before the impact of a vehicle and the maximum lateral position of any major part of the barrier after the impact (Fig. 5). The standard distinguishes between eight classes of deformation of the restraint barrier (W1 to W8).



Sl. 5. Delovna širina (W) cestne varnostne ograje
Fig. 5. Working width (W) of the road restraint barrier

3 IZBIRA PRIMERNE OBLIKE DISTANČNIKA

Obravnavana konstrukcija cestne varnostne ograje (sl. 6a) je izdelana iz konstrukcijskega jekla S 235 (St 37-2 po DIN). Ščitnik je izdelan iz 3 mm debele pločevine in preoblikovan v obliko črke W, ki trdnostne lastnosti še povečuje. Dolžina odbojnika je običajno 4200 mm, pri čemer je dolžina spoja (prekritja) 200 mm. Oporna pločevina je izdelana iz 6 mm debele pločevine in je privarjena na distančnik. Sedanji distančnik je iz profila U, dimenziij 120 x 50 in dolžino 260 mm. Razdalja med oporno pločevino in stebrom znaša 140 mm. Stebri so izdelani iz profila C, izmere 55 x 120 x 4 mm. Praviloma so dolžine 1,9 m. Postavljeni so na medsebojni oddaljenosti 1,33 m, 2 m in 4 m, kar je odvisno od potrebne stopnje zadrževanja vozil. V primeru večje stopnje zadrževanja so razdalje med stebri manjše. V nasprotnem primeru, kadar zadošča manjša stopnja zadrževanja, so lahko razdalje med stebri večje. Steber je postavljen tako, da je zaprti profil obrnjen proti smeri vožnje. Če steba ni mogoče zabititi v zemljino, ga je potrebno s podložno ploščo pritrđiti na sidrno ploščo. Odbojniki, stebri in distančniki so spojeni s pocinkanimi vijaki M16 x 35 mm trdnostnega razreda 5.8.

Pri konstruiranju nove oblike distančnika je bilo treba upoštevati različne zahteve. Distančnik mora biti oblikovan tako, da ograja geometrijsko ustreza državnemu pravilniku o postavitvi cestnih varnostnih ograj. Nadalje mora s svojo obliko čim bolj ublažiti nalet vozila prek akumulacije čim večje količine kinetične energije vozila s svojo nadzorovano elasto-plastično deformacijo.

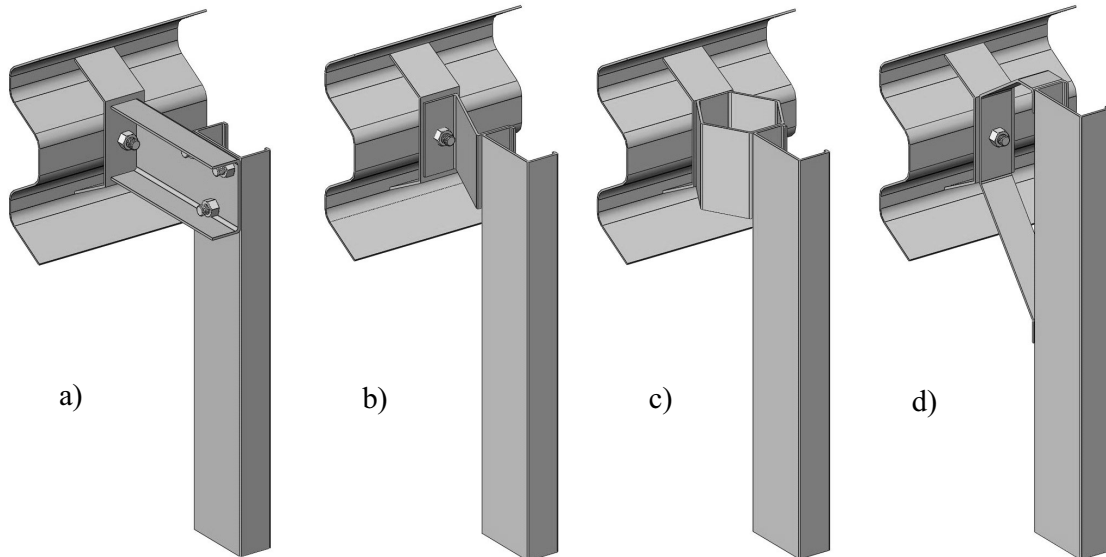
3 SELECTION OF A SUITABLE DISTANCE-SPACER DESIGN

The evaluated road restraint barrier (Fig. 6a) is made of S 235 construction steel (St 37-2 according to DIN). The guardrail is made of 3-mm-thick metal sheet, which is W-shaped to improve its strength characteristics. The usual length of a guardrail segment is 4200 mm; where the splice length is equal to 200 mm. The supporting sheet metal is 6-mm thick and is welded to the distance spacer. The currently used distance spacer is U-shaped with dimensions of 120 mm x 50 mm and 260 mm. The distance between the guardrail and the post is 140 mm. The post is C-shaped with dimensions of 55 mm x 120 mm x 4 mm and it is usually 1900-mm long. The distance between the posts depends on the required containment level and can be 1.33 m, 2 m or 4 m. For higher containment levels the distance between the posts is shorter. In the opposite case, when a lower containment level is required, the distance must be longer. Posts are always oriented with the closed profile towards the direction of traffic flow. If a post cannot be rammed into the soil, it has to be fixed with an anchor-plate. W-beams, posts and distance spacers are joined with standard bolt connections M16 x 35 mm of strength class 5.8.

When designing a new shape of distance spacer, various requirements have to be taken into consideration. The distance spacer has to be designed in such a way that the road restraint barrier geometrically suits the basic regulations. Furthermore, in the event of an impact, it should deform in a controlled manner, thus absorbing as much kinetic energy as possible through elasto-plastic deformation. The dis-

Distančnik mora zagotavljati zadosten odpor silam, ki delujejo nanj, vendar ne sme biti pretog. Pri trku in po njem mora ostati distančnik ves čas povezan s ščitnikom ali stebrom. Distančnik mora biti preprost za izdelavo in montažo in omogočati mora stalno in preprosto vzdrževanje.

Obravnavane so bile štiri različne oblike distančnikov, ki so prikazane na sliki 6.



Sl. 6. Različne oblike distančnikov:

a – profil U (prvotni distančnik); b – profil Z; c – šestkotni profil; d – profil D

Fig. 6. Different distance spacer designs:

a – U profile (current distance spacer); b – Z profile; c – hexagonal profile; d – D profile

4 PRIMERJALNA ANALIZA DISTANČNIKOV PO METODI KONČNIH ELEMENTOV

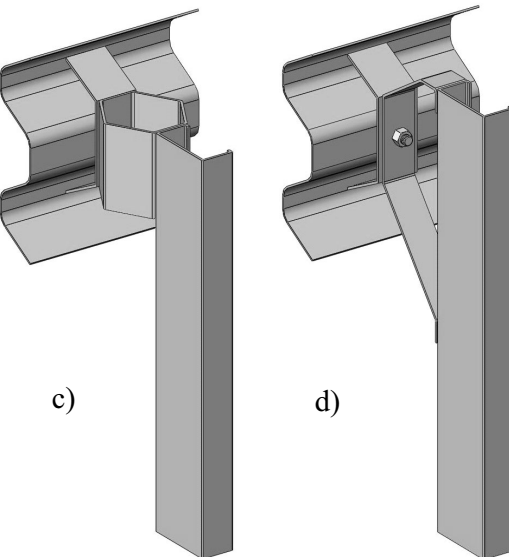
Vsi sestavni deli varnostne ograje so izdelani iz konstrukcijskega jekla S 235. Z namenom, da bi ugotovili materialne lastnosti pločevin različnih debelin, so bili izvedeni natezni preizkusi preskušancev iz jeklene pločevine v skladu s standardom DIN 50115. Iz eksperimentalno dobljenih rezultatov so bile določene elasto-plastične lastnosti materiala (modul elastičnosti, meja plastičnosti in modul plastičnosti), ki so bile uporabljene v bilinearnem elasto-plastičnem modelu materiala pri računalniških simulacijah. Izmerjene materialne lastnosti so podane v preglednici 1.

Računalniški model cestne varnostne naprave je sestavljen iz naslednjih elementov:

- ščitnika: modeliran z linearimi lupinskimimi štirikotnimi elementi, debeline 3 mm;
- oporne pločevine: modelirana z linearimi lupinskimimi štirikotnimi elementi, debeline 6 mm;
- distančnika: modeliran z linearimi lupinskimimi štirikotnimi elementi, debeline 4 mm (razen profil D = 5 mm);
- stebra: modeliran z linearimi lupinskimimi štirikotnimi elementi, debeline 4 mm;

tance spacer must provide enough resistance to the impacting forces but should not be too stiff. It has to stay connected to the guardrail or the post during and after an impact. It also has to be easy and cheap to produce, simple enough to assemble and it should allow permanent and simple maintenance.

Four different distance spacer designs were investigated (Fig. 6).



4 COMPARATIVE ANALYSES WITH THE FINITE-ELEMENT METHOD

All the parts of the road restraint barrier are made of S 235 construction steel. To acquire the appropriate material properties for sheet metal with different thicknesses, standard tension tests were carried out on specimens according to DIN 50115. The required material properties (Young's modulus, yield stress and plasticity modulus) were determined from analyses of the obtained experimental data and were used in the isotropic bilinear elasto-plastic material model in the computational analyses. The measured material properties are listed in Table 1.

The computational model of the road restraint barrier was composed of the following components:

- the guardrail: discretised with linear rectangular shell elements of 3-mm thickness;
- the supporting sheet metal: discretised with linear rectangular shell elements of 6-mm thickness;
- the distance spacer: discretised with linear rectangular shell elements of 4-mm thickness (only the D profile is made of 5-mm-thick sheet metal);
- the post: discretised with linear rectangular shell

Preglednica 1. Materialne lastnosti jeklenih pločevin iz jekla S 235

Table 1. Material properties of sheet metals made of S 235 steel

Debelina pločevine Sheet metal thickness	Modul elastičnosti Young's modulus	Poissonovo število Poisson's ratio	Meja plastičnosti Yield stress	Modul plastičnosti Plasticity modulus	Natezna trdnost Tensile strength
mm	MPa	/	MPa	MPa	MPa
3	190000	0,29	285	696	400
4	200000	0,29	330	969	450
6	210000	0,29	380	1200	480

- vijačnih spojev: v začetni fazi raziskav so vijaki modelirani s togimi končnimi elementi, ki pomenijo vijačne zveze;
- zvarnih spojev: modelirani s togimi elementi.

Povprečna velikost štirikotnih lupinskih elementov je 10 mm. Celoten model je sestavljen iz približno 3200 končnih elementov.

Pri določanju robnih pogojev smo si pomagali s standardom SIST EN 1317, kjer smo za obremenitev v začetni fazi raziskave določili silo trka $F = 30 \text{ kN}$. Ta konzervativna sila je bila enakomerno porazdeljena na dotikalno površino ščitnika v dolžini 300 mm (sl. 7). Celotno konstrukcijo smo toga vpeli na spodnjem delu stebra po robu 3 (sl. 7). Ščitniku smo po robu 1 in 2 predpisali periodične simetrične robne pogoje (sl. 7).

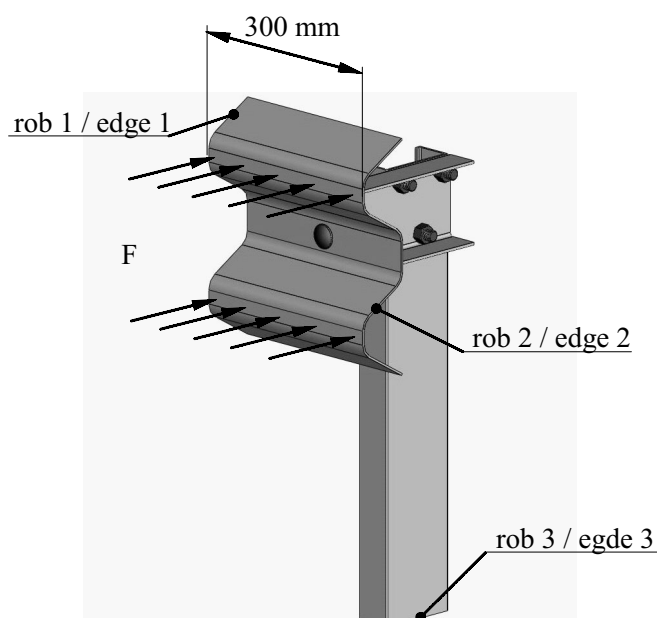
Za izdelavo mreže končnih elementov in nelinearne analize je bil uporabljen programski paket MSC.visualNastran za Windows. Konvergenca rešitve je bila zagotovljena pri 10 do

- elements of 4-mm thickness;
- bolts: the bolt connections were modelled with rigid finite elements;
- welds: the weld connections were modelled with rigid finite elements.

The average size of the rectangular shell elements is 10 mm. The whole model consists of approximately 3200 finite elements.

The loading was defined according to the standard SIST EN 1317, where a constant impact force of 30 kN was evenly distributed along the guardrail contact surface (Fig. 7), 300 mm in length. The post was fixed at the lower part on the edge 3 (Fig. 7) and periodic symmetry boundary conditions were defined at both ends of the guardrail – edges 1 and 2 (Fig. 7).

The MSC.visualNastran for Windows FE system was used for pre-processing, nonlinear analyses and post-processing of the computational results. To obtain a convergent solution it was necessary to

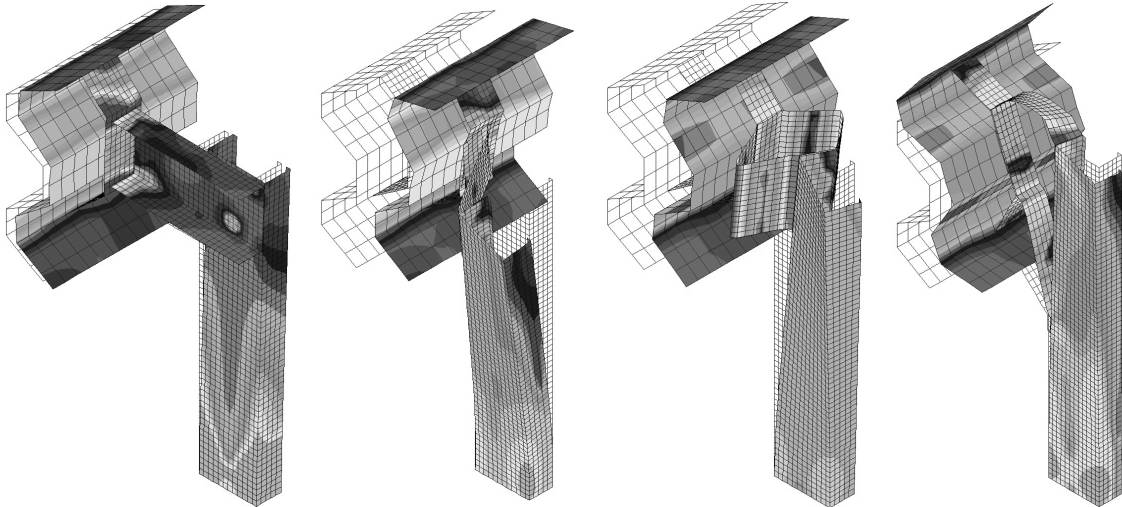


Sl. 7. Robni pogoji
Fig. 7. Boundary conditions

50 obremenitvenih korakih, s 25 iteracijami znotraj koraka ob toleranci obremenitve in dela, ki je znašala 10^{-5} . Uporabljena je bila metoda posodobitve togostne matrike po prvi iteraciji v posameznem koraku obremenitve.

5 PRIMERJAVA REZULTATOV

Rezultati računalniških analiz v obliki pomikov ograje so prikazani na sliki 8.



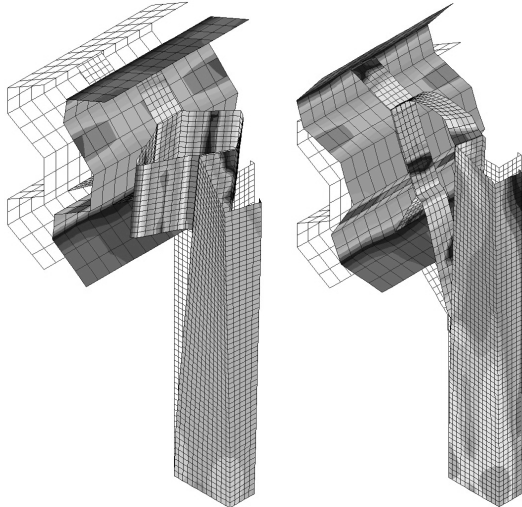
Sl. 8. Pomik cestne varnostne ograje pod obremenitvijo
Fig. 8. The displacement of the road restraint barrier under an applied load

Pri vrednotenju rezultatov so bili najpomembnejši pomiki v smeri delovanja sil, ki ponazarjajo deformacijo ograje pri naletu vozila. Za vrednotenje jakosti udarca je pomembna tudi deformacijska energija, ki jo sprejme konstrukcija varnostne ograje (sl. 9).

define 10–50 load increments and a maximum of 25 iterations inside one load increment. The work and load convergence tolerances were set to a value of 10^{-5} . The stiffness matrix was updated after the first iteration in each load increment.

5 COMPARISON OF THE RESULTS

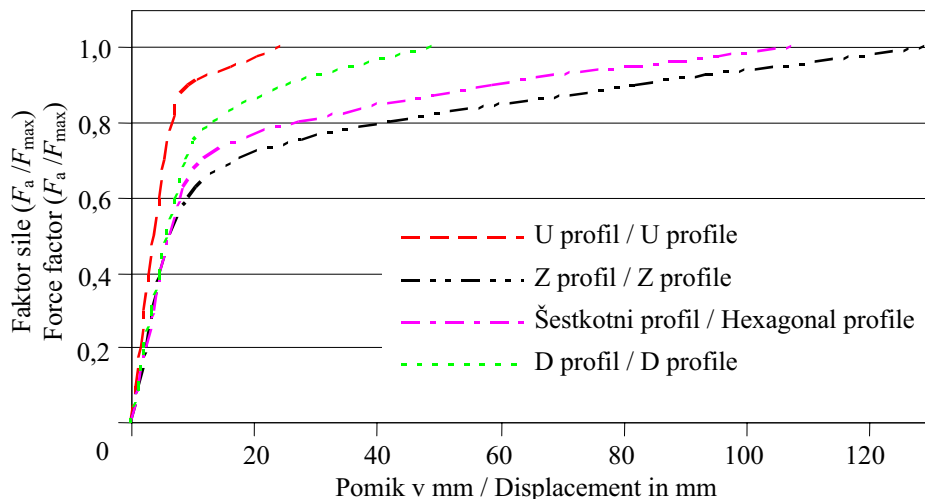
The results of the computational analyses in the form of barrier displacements are shown in Fig. 8.



Sl. 9. Diagram sila – pomik

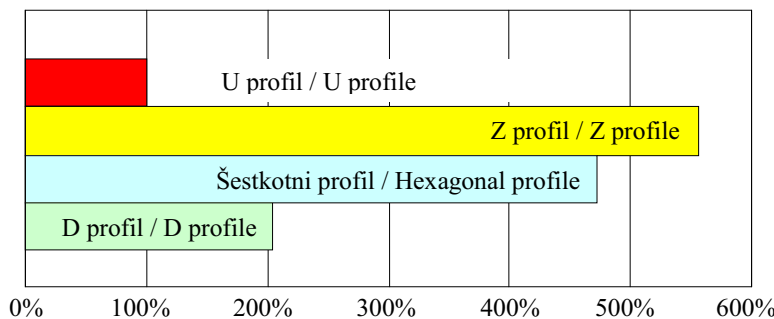
Fig. 9. Force – displacement diagram

The most important data in the process of evaluating the results were the displacements in the direction of the acting forces, which illustrate the deformation of the road restraint barrier in the event of a vehicle impact. When evaluating the impact severity, it is important to consider the strain energy that is absorbed by the safety barrier (Fig. 9).



Sl. 9. Diagram sila – pomik

Fig. 9. Force – displacement diagram



Sl. 10. Primerjava akumulirane deformacijske energije
Fig. 10. Comparison of the strain-energy absorption

Diagram na sliki 10 prikazuje normirane vrednosti akumulirane deformacijske energije, pri čemer znaša izhodiščna vrednost sedanjega distančnika 100%.

Razvidno je, da se trenutni distančnik najmanj deformira, kar ima za posledico zelo velike pojemeke pri naletu vozila v ograjo. Tudi zmožnost akumuliranja deformacijske energije kaže na zelo togo konstrukcijo, ki ne more zagotovljati najboljše varnosti na cestišču. Največji pomik in največjo zmožnost akumuliranja deformacijske energije dosežemo z distančnikom profila Z, vendar je ta deformacija precej nestabilna zaradi nesimetrične oblike distančnika. Najbolj nadzorovano se deformira distančnik v obliki šestkotnika. Njegova zmožnost akumuliranja deformacijske energije je 4,8-krat večja od akumulirane deformacijske energije sedanjega distančnika. Distančnik v obliki črke D je dosegel najslabše rezultate. Dobra lastnost tega distančnika je v tem, da potisne ščitnik navzgor in s tem prepreči, da bi ga vozilo prevozilo. Primerjava rezultatov računalniških simulacij je podana v preglednici 2.

Primerjava rezultatov dokazuje, da sedanji distančnik ne zadovoljuje vseh pogojev uporabe. Ugotovljeno je bilo, da lahko z drugačnimi oblikami distančnikov povečamo zmožnost akumuliranja deformacijske energije in tako posledično

The diagram in Figure 10 shows normalized values of the absorbed strain energy. The value of the currently used distance spacer is 100%.

It is obvious that the currently used distance spacer has the smallest deformation and consequently causes the highest decelerations during vehicle impact. The amount of strain-energy absorption indicates that this design is very stiff and cannot assure proper highway safety. The Z-shaped distance spacer experiences large deformations and higher strain-energy absorption. However, its deformation is very unpredictable due to its non-symmetrical shape. The deformation of the hexagon-shaped distance spacer proved to be the most controllable. Its energy absorption is 4.8 times higher than the strain-energy absorption of the currently used distance spacer. The D-shaped distance spacer has the worst overall performance. However, its major advantage is that it pushes the guardrail up during impact, which prevents the vehicle from overrunning the guardrail. A comparison of the computational analyses results is shown in Table 2.

A comparison of the computational results shows that the currently used distance spacer does not fulfil all the conditions. We found that the use of different distance-spacer designs could increase the strain-energy absorption and consequently decrease the

Preglednica 2. Primerjava rezultatov simulacij
Table 2. Comparison of the computational results

Distančnik Distance spacer	Pomik v prečni smeri Lateral displacement	Največja primerjalna napetost Maximum equivalent stress
	mm	MPa
profil U / U profile	24,1	402
profil Z / Z profile	129,9	480
šestkotni profil / hexagonal profile	108,1	510
profil D / D profile	48,6	480

zmanjšamo pojeme, ki jih pri trku utrpijo potniki v vozilu.

6 SKLEP

Za vrednotenje različnih oblik distančnikov so bile izvedene nelinearne navidezstatične analize odseka cestne varnostne ograje ob upoštevanju naleta osebnega vozila.

Iz rezultatov računalniških simulacij je razvidno, da lahko z drugačnimi oblikami distančnikov zmanjšamo togost varnostne ograje, omogočimo večjo zmožnost deformiranja in tako posredno zmanjšamo pojeme pri naletu vozila ter povečamo varnost potnikov v vozilu.

Rezultati računalniških simulacij dokazujejo, da je dosedanji distančnik pretog in je očitno konstruiran zgolj po geometrijskih pravilih, ne glede na funkcionalnost. Najboljše rezultate dosegata distančnika oblike Z in šestkotnega profila. Čeprav ima distančnik iz profila Z manjšo togost in večjo zmožnost akumuliranja deformacijske energije, se distančnik iz šestkotnega profila deformira bolj predvidljivo in zaradi svoje simetričnosti ni občutljiv na kot naleta vozila na ograjo.

V nadaljnjih raziskavah bo simuliran dinamični nalet realnega vozila na varnostno ograjo (sl. 11), pri čemer bo upoštevana tudi deformacija podlage, v katero so nameščeni stebri.

decelerations experienced by the vehicle occupants during an impact.

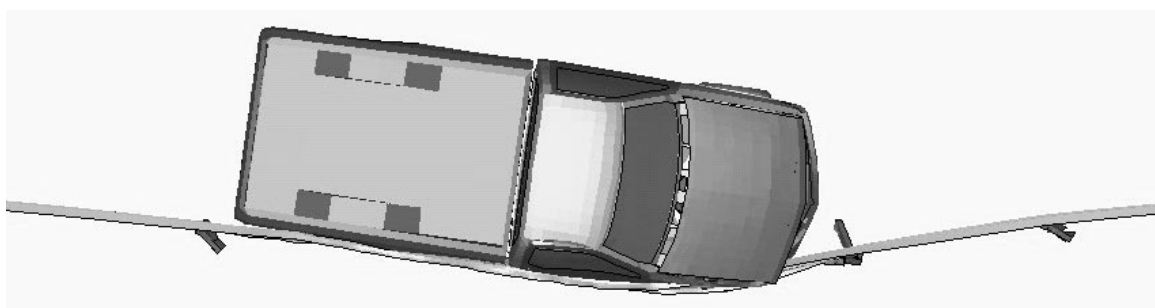
6 CONCLUSION

The nonlinear quasi-static analyses of a segment of road restraint barrier under vehicle-impact conditions were carried out to evaluate a variety of distance-spacer designs.

The results of the computational analyses show that it is possible to reduce the stiffness of the road restraint barrier and increase its ability to absorb energy by using a range of distance-spacer designs, thus reducing the deceleration of an impacting vehicle and consequently increasing the safety of the vehicle occupants.

The computational simulations showed that the current distance spacer is far too stiff and was obviously designed only according to geometrical rules, and not according to its functionality. Better results can be achieved by using a Z-shaped or hexagon-shaped distance spacer. Although the Z profile has a lower stiffness and a higher strain-energy absorption capability, the hexagonal profile deforms in a more predictable way and is not sensitive to the vehicle impacting angle, due to its symmetry.

It is intended to continue this research with fully transient dynamic analyses of the road restraint barrier under real vehicle-impact conditions (Fig. 11). The soil deformation will also be taken into consideration during subsequent computational simulations of the road restraint barrier.



Sl. 11. Dinamična simulacija cestne varnostne ograje
Fig. 11. Dynamic simulation of the road restraint barrier

7 LITERATURA

7 REFERENCES

- [1] Engstrand, K. E. (2000) Improvements to the weak - post w - beam guardrail. Worcester: Worcester Polytechnic Institute.
- [2] European Committee for Standardization. (1998) European Standard EN 1317-1, EN 1317-2, Road Restraint Systems.
- [3] Nafems (1992) Nafems - introduction to nonlinear finite element analysis, *Nafems Birniehill*, Glasgow.
- [4] Ministrstvo za promet (2001) Tehnična specifikacija za javne ceste. Urad za standardizacijo in meroslovje. Direkcija republike Slovenije za ceste. TSC 02.xxx, Varnostne ograje, pogoji in načini postavitve.
- [5] Vesenjak, M., Z. Ren (2002) Konstruiranje distančnika cestne varnostne ograje. Kuhljevi dnevi '02, Ribno pri Bledu, 26.-27. september 2002. *Zbornik del. Ljubljana: Slovensko društvo za mehaniko*.
- [6] Železarna Jesenice (1974) Cestna varnostna ograja, Kranj.

Naslov avtorjev: Matej Vesenjak
prof.dr. Zoran Ren
Univerza v Mariboru
Fakulteta za strojništvo
Smetanova 17
2000 Maribor
m.vesenjak@uni-mb.si
ren@uni-mb.si

Author's Address: Matej Vesenjak
Prof.Dr. Zoran Ren
University of Maribor
Faculty of Mechanical Eng.
Smetanova 17
2000 Maribor, Slovenia
m.vesenjak@uni-mb.si
ren@uni-mb.si

Prejeto:
Received: 20.8.2003

Sprejeto:
Accepted: 18.12.2003

Odprto za diskusijo: 1 leto
Open for discussion: 1 year

Osebne vesti Personal Events

Doktorati, specializacije, diplome

DOKTORATI

Na Fakulteti za strojništvo Univerze v Ljubljani so z uspehom zagovarjali svoje doktorske disertacije, in sicer:

dne 9. oktobra 2003: **mag. Viktor Šajn**, z naslovom: "Optimiranje oblike profila deformabilnega letalskega krila glede na aerodinamične sile";

dne 15. oktobra 2003: **mag. Boris Kuselj**, z naslovom: "Razslojevanje in lokalno izbočenje večslojnih plošč";

dne 28. oktobra 2003: **mag. Gorazd Hlebanja**, z naslovom: "Raziskava matematičnega modela za dimenzioniranje drsnih površin pri hladnem zajedanju".

Na Fakulteti za strojništvo Univerze v Mariboru so z uspehom zagovarjali svoje doktorske disertacije, in sicer:

dne 20. oktobra 2003: **mag. Matjaž Milfelner**, z naslovom: "Spremljanje in optimiranje procesa frezanja z oblikovnim krogelnim frezalom z uporabo genetskih algoritmov";

dne 23. oktobra 2003: **mag. Marjan Delić**, z naslovom: "Numerično modeliranje tokov pastastih snovi";

dne 29. oktobra 2003: **mag. Mitja Kastrevc**, z naslovom: "Analiza dinamike pogonske zveze asinhronskega elektromotorja in hidravlične zobniške črpalke".

S tem so navedeni kandidati dosegli akademsko stopnjo doktorja znanosti.

SPECIALIZACIJE

Na Fakulteti za strojništvo Univerze v Mariboru je z uspehom zagovarjal svoje specialistično delo, in sicer:

dne 13. oktobra 2003: **Matjaž Aberšek**, z naslovom: "Projekt postavitve proizvodnje avtomobilskih vzglavnikov".

S tem je navedeni kandidat dosegel stopnjo specialista.

DIPLOMIRALI SO

Na Fakulteti za strojništvo Univerze v Ljubljani so pridobili naziv diplomirani inženir strojništva:

dne 9. oktobra 2003: Alen BOGATAJ, Matej JELOVČAN, Dejan KREK, Jože LUŽAR, Jože MOLEK, Primož ŠUŠTERŠIČ, Tomaž TOPOLŠEK;

dne 10. oktobra 2003: Rok DOBRAVC, Marko FIJAVŽ, Primož JOVANOVIĆ, Ervin KROPIVŠEK, Robert NOVAK;

dne 13. oktobra 2003: Mitja LIPOVŠEK, Matej MLAKAR, Zorislav NEDELJKOVIĆ, Roman OSOLNIK, Marino PLEVANČ, Simon ŠIFRAR.

Na Fakulteti za strojništvo Univerze v Mariboru so pridobili naziv diplomirani inženir strojništva:

dne 29. oktobra 2003: Aleksander DRAKSLER, Denis LINDIČ, Aleksander ŠCANČAR, Andrej ZUPAN;

dne 30. oktobra 2003: Matej KOLETNIK, Marjan PINTARIČ, Dejan PURNAT, David ŠOŠTARIČ.

Navodila avtorjem

Instructions for Authors

Članki morajo vsebovati:

- naslov, povzetek, besedilo članka in podnaslove slik v slovenskem in angleškem jeziku,
- dvojezične preglednice in slike (diagrami, risbe ali fotografije),
- seznam literature in
- podatke o avtorjih.

Strojniški vestnik izhaja od leta 1992 v dveh jezikih, tj. v slovenščini in angleščini, zato je obvezen prevod v angleščino. Obe besedili morata biti strokovno in jekovno med seboj usklajeni. Članki naj bodo kratki in naj obsegajo približno 8 tipkanih strani. Izjemoma so strokovni članki, na željo avtorja, lahko tudi samo v slovenščini, vsebovati pa morajo angleški povzetek.

Vsebina članka

Članek naj bo napisan v naslednji obliki:

- Naslov, ki primerno opisuje vsebino članka.
- Povzetek, ki naj bo skrajšana oblika članka in naj ne presega 250 besed. Povzetek mora vsebovati osnove, jedro in cilje raziskave, uporabljeno metodologijo dela, povzetek rezultatov in osnovne sklepe.
- Uvod, v katerem naj bo pregled novejšega stanja in zadostne informacije za razumevanje ter pregled rezultatov dela, predstavljenih v članku.
- Teorija.
- Eksperimentalni del, ki naj vsebuje podatke o postavitev preskusa in metode, uporabljene pri pridobitvi rezultatov.
- Rezultati, ki naj bodo jasno prikazani, po potrebi v obliki slik in preglednic.
- Razprava, v kateri naj bodo prikazane povezave in pospološtive, uporabljene za pridobitev rezultatov. Prikazana naj bo tudi pomembnost rezultatov in primerjava s poprej objavljenimi deli. (Zaradi narave posameznih raziskav so lahko rezultati in razprava, za jasnost in preprostejše bralčev razumevanje, združeni v eno poglavje.)
- Sklepi, v katerih naj bo prikazan en ali več sklepov, ki izhajajo iz rezultatov in razprave.
- Literatura, ki mora biti v besedilu oštevilčena zaporedno in označena z oglatimi oklepaji [1] ter na koncu članka zbrana v seznamu literature. Vse opombe naj bodo označene z uporabo dvignjene številke¹.

Oblika članka

Besedilo naj bo pisano na listih formata A4, z dvojnim presledkom med vrstami in s 3 cm širokim robom, da je dovolj prostora za popravke lektorjev. Najbolje je, da pripravite besedilo v urejevalniku Microsoft Word. Hkrati dostavite odtis članka na papirju, vključno z vsemi slikami in preglednicami ter identično kopijo v elektronski obliki.

Prosimo, da ne uporabljate urejevalnika LaTeX, saj program, s katerim pripravljamo Strojniški vestnik, ne uporablja njegovega formata. V urejevalniku LaTeX oblikujte grafe, preglednice in enačbe in jih stiskajte na kakovosten laserskem tiskalniku, da jih bomo lahko presneli.

Enačbe naj bodo v besedilu postavljene v ločene vrstice in na desnem robu označene s tekočo številko v okroglih oklepajih

Enote in okrajšave

V besedilu, preglednicah in slikah uporabljajte le standardne označbe in okrajšave SI. Simbole fizikalnih veličin v besedilu pišite poševno (kurzivno), (npr. *v*, *T*, *n* itn.). Simbole enot, ki sestojijo iz črk, pa pokončno (npr. ms^{-1} , K, min, mm itn.).

Vse okrajšave naj bodo, ko se prvič pojavijo, napisane v celoti v slovenskem jeziku, npr. časovno spremenljiva geometrija (CSG).

Papers submitted for publication should comprise:

- Title, Abstract, Main Body of Text and Figure Captions in Slovene and English,
- Bilingual Tables and Figures (graphs, drawings or photographs),
- List of references and
- Information about the authors.

Since 1992, the Journal of Mechanical Engineering has been published bilingually, in Slovenian and English. The two texts must be compatible both in terms of technical content and language. Papers should be as short as possible and should on average comprise 8 typed pages. In exceptional cases, at the request of the authors, speciality papers may be written only in Slovene, but must include an English abstract.

The format of the paper

The paper should be written in the following format:

- A Title, which adequately describes the content of the paper.
- An Abstract, which should be viewed as a miniversion of the paper and should not exceed 250 words. The Abstract should state the principal objectives and the scope of the investigation, the methodology employed, summarize the results and state the principal conclusions.
- An Introduction, which should provide a review of recent literature and sufficient background information to allow the results of the paper to be understood and evaluated.
- A Theory
- An Experimental section, which should provide details of the experimental set-up and the methods used for obtaining the results.
- A Results section, which should clearly and concisely present the data using figures and tables where appropriate.
- A Discussion section, which should describe the relationships and generalisations shown by the results and discuss the significance of the results making comparisons with previously published work. (Because of the nature of some studies it may be appropriate to combine the Results and Discussion sections into a single section to improve the clarity and make it easier for the reader.)
- Conclusions, which should present one or more conclusions that have been drawn from the results and subsequent discussion.
- References, which must be numbered consecutively in the text using square brackets [1] and collected together in a reference list at the end of the paper. Any footnotes should be indicated by the use of a superscript¹.

The layout of the text

Texts should be written in A4 format, with double spacing and margins of 3 cm to provide editors with space to write in their corrections. Microsoft Word for Windows is the preferred format for submission. One hard copy, including all figures, tables and illustrations and an identical electronic version of the manuscript must be submitted simultaneously.

Please do not use a LaTeX text editor, since this is not compatible with the publishing procedure of the Journal of Mechanical Engineering. Graphs, tables and equations in LaTeX may be supplied in good quality hard-copy format, so that they can be copied for inclusion in the Journal.

Equations should be on a separate line in the main body of the text and marked on the right-hand side of the page with numbers in round brackets.

Units and abbreviations

Only standard SI symbols and abbreviations should be used in the text, tables and figures. Symbols for physical quantities in the text should be written in Italics (e.g. *v*, *T*, *n*, etc.). Symbols for units that consist of letters should be in plain text (e.g. ms^{-1} , K, min, mm, etc.).

All abbreviations should be spelt out in full on first appearance, e.g., variable time geometry (VTG).

Slike

Slike morajo biti zaporedno oštevilčene in označene, v besedilu in podnaslovu, kot sl. 1, sl. 2 itn. Posnete naj bodo v kateremkoli od razširjenih formatov, npr. BMP, JPG, GIF. Za pripravo diagramov in risb priporočamo CDR format (CorelDraw), saj so slike v njem vektorske in jih lahko pri končni obdelavi preprosto povečujemo ali pomanjšujemo.

Pri označevanju osi v diagramih, kadar je le mogoče, uporabite označbe veličin (npr. t , v , m itn.), da ni potrebno dvojezično označevanje. V diagramih z več krivuljami, mora biti vsaka krivulja označena. Pomen oznake mora biti pojasnjен v podnapisu slike.

Vse označbe na slikah morajo biti dvojezične.

Za vse slike po fotografiskih posnetkih je treba priložiti izvirne fotografije ali kakovostno narejen posnetek. V izjemnih primerih so lahko slike tudi barvne.

Preglednice

Preglednice morajo biti zaporedno oštevilčene in označene, v besedilu in podnaslovu, kot preglednica 1, preglednica 2 itn. V preglednicah ne uporabljajte izpisanih imen veličin, ampak samo ustrezne simbole, da se izognemo dvojezični podvojitvi imen. K fizikalnim veličinam, npr. t (pisano poševno), pripisite enote (pisano pokončno) v novo vrsto brez oklepajev.

Vsi podnaslovi preglednic morajo biti dvojezični.

Seznam literature

Vsa literatura mora biti navedena v seznamu na koncu članka v prikazani obliki po vrsti za revije, zbornike in knjige:

- [1] Targ, Y.S., Y.S. Wang (1994) A new adaptive controller for constant turning force. *Int J Adv Manuf Technol* 9(1994) London, pp. 211-216.
- [2] Čuš, F., J. Balić (1996) Rationale Gestaltung der organisatorischen Abläufe im Werkzeugwesen. *Proceedings of International Conference on Computer Integration Manufacturing*, Zakopane, 14.-17. maj 1996.
- [3] Oertli, P.C. (1977) Praktische Wirtschaftskybernetik. *Carl Hanser Verlag*, München.

Podatki o avtorjih

Članku priložite tudi podatke o avtorjih: imena, nazive, popolne poštne naslove, številke telefona in faks ter naslove elektronske pošte.

Sprejem člankov in avtorske pravice

Uredništvo Strojniškega vestnika si pridržuje pravico do odločanja o sprejemu članka za objavo, strokovno oceno recenzentov in morebitnem predlogu za krajšanje ali izpopolnitve ter terminološke in jezikovne korekturje.

Avtor mora predložiti pisno izjavo, da je besedilo njegovo izvirno delo in ni bilo v dani obliki še nikjer objavljeno. Z objavo preidejo avtorske pravice na Strojniški vestnik. Pri morebitnih kasnejših objavah mora biti SV naveden kot vir.

Rokopisi člankov ostanejo v arhivu SV.

Vsa nadaljnja pojasnila daje:

Uredništvo
STROJNISKEGA VESTNIKA
p.p. 197
1001 Ljubljana
Telefon: (01) 4771-757
Telefaks: (01) 2518-567
E-mail: strojniski.vestnik@fs.uni-lj.si

Figures

Figures must be cited in consecutive numerical order in the text and referred to in both the text and the caption as Fig. 1, Fig. 2, etc. Figures may be saved in any common format, e.g. BMP, GIF, JPG. However, the use of CDR format (CorelDraw) is recommended for graphs and line drawings, since vector images can be easily reduced or enlarged during final processing of the paper.

When labelling axes, physical quantities, e.g. t , v , m , etc. should be used whenever possible to minimise the need to label the axes in two languages. Multi-curve graphs should have individual curves marked with a symbol, the meaning of the symbol should be explained in the figure caption.

All figure captions must be bilingual.

Good quality black-and-white photographs or scanned images should be supplied for illustrations. In certain circumstances, colour figures may be considered.

Tables

Tables must be cited in consecutive numerical order in the text and referred to in both the text and the caption as Table 1, Table 2, etc. The use of names for quantities in tables should be avoided if possible: corresponding symbols are preferred to minimise the need to use both Slovenian and English names. In addition to the physical quantity, e.g. t (in Italic), units (normal text), should be added in new line without brackets.

All table captions must be bilingual.

The list of references

References should be collected at the end of the paper in the following styles for journals, proceedings and books, respectively:

- [1] Targ, Y.S., Y.S. Wang (1994) A new adaptive controller for constant turning force. *Int J Adv Manuf Technol* 9(1994) London, pp. 211-216.
- [2] Čuš, F., J. Balić (1996) Rationale Gestaltung der organisatorischen Abläufe im Werkzeugwesen. *Proceedings of International Conference on Computer Integration Manufacturing*, Zakopane, 14.-17. maj 1996.
- [3] Oertli, P.C. (1977) Praktische Wirtschaftskybernetik. *Carl Hanser Verlag*, München.

Author information

The following information about the authors should be enclosed with the paper: names, complete postal addresses, telephone and fax numbers and E-mail addresses.

Acceptance of papers and copyright

The Editorial Committee of the Journal of Mechanical Engineering reserves the right to decide whether a paper is acceptable for publication, obtain professional reviews for submitted papers, and if necessary, require changes to the content, length or language.

Authors must also enclose a written statement that the paper is original unpublished work, and not under consideration for publication elsewhere. On publication, copyright for the paper shall pass to the Journal of Mechanical Engineering. The JME must be stated as a source in all later publications.

Papers will be kept in the archives of the JME.

You can obtain further information from:

Editorial Board of the
JOURNAL OF MECHANICAL ENGINEERING
P.O.Box 197
1001 Ljubljana, Slovenia
Telephone: +386 (0)1 4771-757
Fax: +386 (0)1 2518-567
E-mail: strojniski.vestnik@fs.uni-lj.si